NEW YORK UNIVERSITY
INSTITUTE OF MATHEMATICAL SCIENCES
LIBRARY
25 Waverly Place, New York 3, N. Y.

AFCRC-TN-59-390

NEW YORK UNIVERSITY
Institute of Mathematical Sciences
Division of Electromagnetic Research

RESEARCH REPORT No. EM-136

Structure of the Electromagnetic Field in the Image Region of an Aplanatic Optical System

E. WOLF and B. RICHARDS

Contract No. AF 19(604)5238

JULY, 1959

EM-136
c.1

AFCRC-TN-59-390

NEW YORK UNIVERSITY

Institute of Mathematical Sciences
Division of Electromagnetic Research

Research Report No. EM-136

Structure of the Electromagnetic Field in the Image Region of an Aplanatic Optical System

E. Wolf and B. Richards

E. Wolf

B. Richards

Sidney Borowitz
Acting Director

Werner Gerbes
Contract Monitor

The research reported in this document has been sponsored in part by the Electronics Research Directorate of the Air Force Cambridge Research Center, Air Research and Development Command.

Contract No. AF 19(604)5238

July, 1959

Requests for additional copies by Agencies of the Department of Defense, their contractors, and other Government agencies should be directed to the:

ARMED SERVICES TECHNICAL INFORMATION AGENCY
DOCUMENTS SERVICE CENTER
ARLINGTON HALL STATION
ARLINGTON 12, VIRGINIA

Department of Defense contractors must be established for ASTIA services or have their 'need-to-know' certified by the cognizant military agency of their project or contract.

All other persons and organizations should apply to the:

U.S. DEPARTMENT OF COMMERCE
OFFICE OF TECHNICAL SERVICES
WASHINGTON 25, D.C.

ABSTRACT

An investigation is made of the structure of the electromagnetic field near the focus of an aplanatic system which images a point source. First the case of a linearly polarized incident field is examined and expressions are derived for the electric and magnetic vectors in the image space. Some general consequences of the formulas are then discussed. In particular the symmetry properties of the field with respect to the focal plane are noted and the state of polarization of the image region is investigated. The distribution of the time averaged electric and magnetic energy densities and of the energy flow (Poynting vector) in the focal plane is studied in detail and the results are illustrated by diagrams and in a tabulated form based on data obtained by extensive calculations on an electronic computer. The case of an unpolarized field is also investigated.

The solution is not restricted to systems of low aperture, and the computational results cover, in fact, selected values of the angular semi-aperture α on the image side, in the whole range $0 \leq \alpha \leq 90^{\circ}$. The limiting case $\alpha \rightarrow 0$ is examined in detail and it is shown that the field is then completely characterized by a single, generally complex, scalar function, which turns out to be identical with that of the classical scalar theory of Airy, Lommel and Struve.

The results have an immediate bearing on the resolving power of image forming systems; they also help to understand the significance of the scalar diffraction theory, which is customarily employed without proper justification, in the analysis of images in low aperture systems.

Table of Contents

		Page
1.	Introduction	1
2.	Expressions for the field vectors in the image space of an aplanatic system	2
3.	The image field	13
	3.1 Polarization of the image field	16
	3.2 The energy density	18
	3.3 The energy flow (Poynting vector)	23
4.	Approximate form of the solution for systems with a small angular aperture	29
5.	Images formed by an unpolarized wave	33
	References	40

1. Introduction

A knowledge of the structure of an electromagnetic field in the region of focus is of considerable theoretical as well as practical interest. As already indicated in a previous report [Wolf,1958], information about the structure of this complex region is particularly desirable in connection with the design and the analysis of performance of optical systems of wide angular aperture, both in the field of visible and microwave optics. The construction of large paraboloids for use in radio astronomy has made this problem also of topical interest.

Apart from the usual scalar treatments, the limitations of which were mentioned in the previous report, the only earlier treatments of this problem appear to be those of Ignatowsky (1919, 1920) and Hopkins (1943, 1945).* The investigations of Ignatowsky have gone a considerable way towards the solution of the problem. He obtained formulas for the electric and magnetic field vectors in the image region of an aplanatic system** and also of a paraboloid of any angular aperture. Unfortunately his deductions from these formulas were chiefly confined to the study of the energy flow across the central bright nucleus of the image; the electric energy (which is presumably what most detectors, e.g. a photographic plate, record) is not discussed. The researches of Hopkins were mainly concerned with the modification which the Airy pattern undergoes as the angular aperture of the system is increased. While his analysis is not based on the full Maxwell's equations, it does take into account the vectorial nature of the problem and his results are of practical interest in connection with optical systems the angular semi-apertures of which do not exceed about 40°.

---

*Since the present investigation was carried out, two related papers appeared. Burtin (1956) determined the distribution of the electric energy density in the focal plane of a system with angular semi-aperture $\alpha = 45^{\circ}$ on the image side, when the wave entering the system is linearly polarized. Focke (1957) considered an unpolarized wave and studied the energy density and the energy flow at points in the focal plane in systems of selected angular apertures.

**By aplanatic system we mean one which, for a specified axial position of the object point, is stigmatic and obeys the Abbe sine condition.

In the present paper a thorough investigation is made of the structure of the electromagnetic field near the focus of an aplanatic system which images a point source at infinity. Formulas are derived for the electric and magnetic vectors in the image space, and a number of general properties of the electromagnetic field are deduced, both for the case of polarized, as well as unpolarized incident waves. The formulas are evaluated for a large number of the basic parameters of the problem and the results are presented in the form of diagrams and in tabulated form. Systems of selected angular semi-aperture α on the image side are considered, up to the limiting case $\alpha \to 90^{\circ}$. The other limiting case, $\alpha \to 0$, is examined in detail and it is found that, in this case, the vector solution is completely characterized by one (generally complex) scalar function, which is found to be identical with that of the classical analyses of Airy (1835), Lommel (1885) and Struve (1886).

The results have an immediate bearing on the resolving power of systems with high angular aperture; they also help our understanding of the significance of the usual scalar methods of optical diffraction theory.

Finally, it may be mentioned that our basic formulas, Equations (2.30) and (2.31), are in agreement with those of Ignatowsky (1919); our deductions go considerably further, however.

Some preliminary results of this investigation were reported in two previous notes [Richards (1956a), Richards and Wolf (1956)].

2. Expressions for the field vectors in the image space of an aplanatic system.

Consider an optical system of revolution which images a point source. The imaging will be assumed to be aplanatic, i.e. axially stigmatic and obeying the sine condition. The source will be assumed to be at infinity in the direction of the axis, and to begin with it will be assumed that the source is monochromatic, and that it gives rise to a linearly polarized wave in the entrance pupil of the system. The case of an unpolarized wave will be considered later (§ 5), by averaging over all possible states of polarization. It is assumed that the linear dimensions of the exit pupil are large compared with the wavelength.

Expressions for the field in the image region of the system may be derived by an application of formulas (2.22) and (2.23) of a previous report [Wolf, 1958]. These formulas express the time independent parts, $\vec{e}$ and $\vec{h}$, of the electric and magnetic vectors

$$(2.1) \qquad \vec{E}(x,y,z,t) = \mathcal{R}\left\{\vec{e}(x,y,z,)e^{-i\omega t}\right\}, \quad \vec{H}(x,y,z,t) = \mathcal{R}\left\{\vec{h}(x,y,z,)e^{-i\omega t}\right\},$$

at any point $P(x,y,z)$ in the image space, which is not too close to the exit pupil, in the form

$$(2.2) \qquad \vec{e}(x,y,z) = -\frac{ik}{2\pi}\iint_{\Omega} \frac{\vec{a}(s_x,s_y)}{s_z} \exp\left\{ik\left[\Phi(s_x,s_y)+s_x x+s_y y+s_z z\right]\right\} ds_x ds_y ,$$

$$(2.3) \qquad \vec{h}(x,y,z) = -\frac{ik}{2\pi}\iint_{\Omega} \frac{\vec{b}(s_x,s_y)}{s_z} \exp\left\{ik\left[\Phi(s_x,s_y)+s_x x+s_y y+s_z z\right]\right\} ds_x ds_y ,$$

where $\mathcal{R}$ denotes the real part. Here $\vec{a}$ and $\vec{b}$ are the 'strength factors' of the unperturbed electromagnetic field $\vec{E}^{(i)} = \mathcal{R}\left\{\vec{e}^{(i)}e^{-i\omega t}\right\}$, $\vec{H}^{(i)} = \mathcal{R}\left\{\vec{h}^{(i)}e^{-\omega t}\right\}$ which is incident on the exit pupil, i.e. $\vec{a}$ and $\vec{b}$ are defined by the relations

$$(2.4) \qquad \vec{e}^{\,(i)} = \frac{\vec{a}}{\sqrt{R_1 R_2}} e^{ik\mathcal{S}}, \qquad \vec{h}^{\,(i)} = \frac{\vec{b}}{\sqrt{R_1 R_2}} e^{ik\mathcal{S}},$$

where R_1 and R_2 are the principal radii of curvature of the associated wavefront and $\mathcal{S}$ is the eikonal function. Further

$$(2.5) \qquad k = \frac{\omega}{c} = \frac{2\pi}{\lambda}$$

is the vacuum number, and λ the vacuum wave length, and it is assumed that the refractive index of the image space is unity. Further Φ is the aberration function of the system, s_x, s_y, s_z are the components of the unit

vector $\vec{s}$ (with its positive direction in the direction of propagation of the light) along a typical ray in the image space, and Ω is the solid angle formed by all the geometrical rays which pass through the exit. pupil of the system. According to Equation (2.24) of the previous report, the strength factors are related by the formula (assuming that in the image space $\epsilon \sim \mu \sim 1$)

$$\vec{b} = \vec{s} \wedge \vec{a} \quad . \tag{2.6}$$

In the problem under consideration, the imaging is aplanatic so that the wavefronts in the image space are spherical, with a common centre at the Gaussian image point. Hence, for all vectors $\vec{s}$ in the solid angle Ω,

$$\Phi (s_x , s_y) = 0 \quad . \tag{2.7}$$

The strength factors $\vec{a}$ and $\vec{b}$ may be determined, with an accuracy sufficient for our purposes, by tracing rays through the system up to the region of the exit pupil, and by making use of the laws relating to the variation of the field vectors along each ray. Let AQ_o be a typical ray entering the system at a height h from the axis and let θ be the angle which the corresponding ray QO in the image space makes with the axis (Figure 1). Since the field in the object space is linearly polarized, the field obtained on refraction at the first surface σ_1 is also linearly polarized*; and if the angle of the incidence at σ_1 is small, the angle which the direction of vibrations of the electric (and also of the magnetic) vector makes with the meridional plane of the ray (the plane containing the ray and the axis of the system) will be effectively unchanged by refraction.**

---

* The direction of polarization will, of course, be, in general, different for different rays.

** The truth of these statements follows from Fresnel formulas for refraction of a plane wave on a plane interface between two homogeneous medis of different refractive indices. Within the accuracy of the present approximation (geometric optics limit, i.e. $k \to \infty$), these formulas also apply to the present case when neither the wavefronts nore the refracting boundaries are necessarily plane.

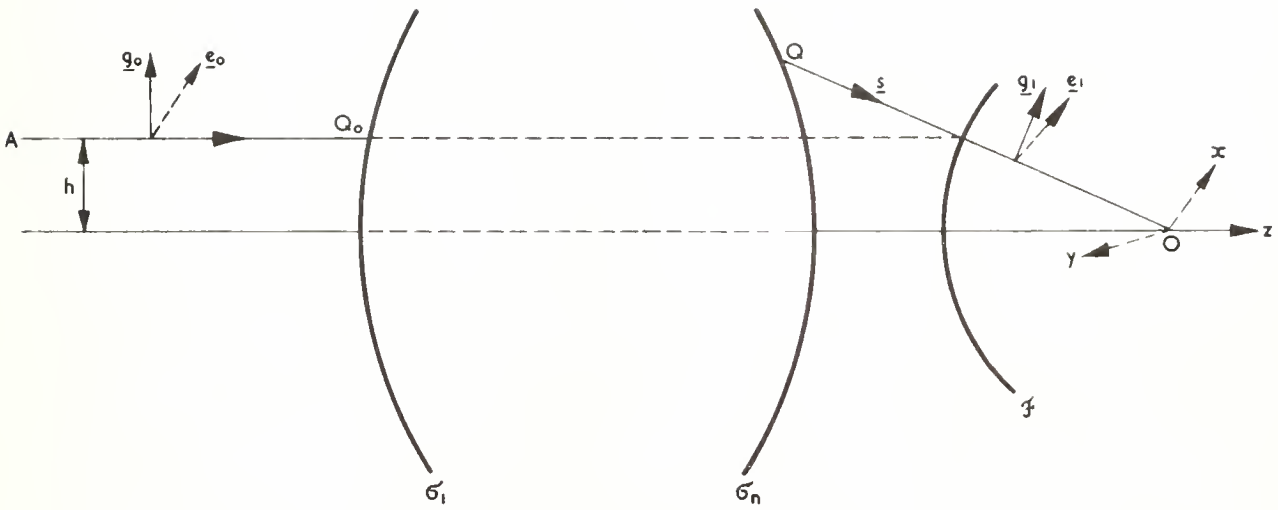

FIGURE 1

For caption to Figure see page 40.

Moreover [see Born and Wolf (1959), § 3.1.3], in an homogeneous medium the direction of vibration remains unchanged along each ray. By successive repetition of these arguments from surface to surface it follows that the field in the region of the exit pupil is also linearly polarized, and that, provided the angle of incidence at each surface of the system is small, the angles which the $\vec{e}$ and $\vec{h}$ vectors in the exit pupil make with the meridional plane of the ray are equal to the corresponding angle in the object space. Further, the magnitude of the field vectors in the region of the exit pupil may be determined from the geometrical law of conservation of energy, taking into account the fact that the system obeys the sine condition.

Let $\mathcal{F}$ be the 'focal sphere', i.e. the sphere with centre at O and with radius f equal to the focal length of the system. Then, according to the sine condition

$$h = f \sin \Theta \,. \tag{2.8}$$

This relation implies that the emergent ray meets the focal sphere at the same height at which the corresponding ray in the object space entered the system (see Figure 1).

Consider now all the rays which enter the annulus bounded by circles of radius h and h + δh. Let δS_o be the area of the annulus and δS_1 be the corresponding area of the focal sphere, and let $\vec{e}_o$ and $\vec{e}_1$ be the electric amplitude vectors on δS_o and δS_1 respectively. Then we may write

$$\vec{e}_o = \ell_o \hat{\vec{e}}_o e^{ik\mathcal{S}_o} \,, \quad \vec{e}_1 = \ell_o \hat{\vec{e}}_1 e^{ik\mathcal{S}_1} \,, \tag{2.9}$$

where $\hat{\vec{e}}_o$ and $\hat{\vec{e}}_1$ are unit vectors, in the direction of $\vec{e}_o$ and $\vec{e}_1$, respectively, ℓ_o and ℓ_1 are amplitude factors and $\mathcal{S}_o$ and $\mathcal{S}_1$ are the corresponding values of the eikonal. Since the field is linearly polarized, ℓ_o, ℓ_1, $\hat{\vec{e}}_o$ and $\hat{\vec{e}}_1$ may be taken to be real, provided that the origin of the phase is suitably chosen.

According to the geometrical optics intensity law,

$$\mathscr{l}_o^2 \delta S_o = \mathscr{l}_1^2 \delta S_1 , \tag{2.10}$$

where we assumed that the refractive index of the object space, like that of the image space is unity, and the losses of energy due to reflection and absorption within the system are negligible. Now from the figure,

$$\delta S_o = \delta S_1 \cos\theta , \tag{2.11}$$

so that according to (2.10)

$$\mathscr{l}_1 = \mathscr{l}_o \sqrt{\cos\theta} . \tag{2.12}$$

Now $\vec{e}_1$ may be identified with the vector $\vec{e}^{(i)}$ of (2.4), with $R_1 = R_2 = f$ and $\mathscr{S} = \mathscr{S}_1$. Hence

$$\vec{a} = f \mathscr{l}_o \sqrt{\cos\theta}\, \hat{\vec{e}}_1 . \tag{2.13}$$

To determine $\hat{\vec{e}}_1$ it is convenient to introduce two unit vectors $\vec{g}_o$ and $\vec{g}_1$ in the meridional plane of the ray, such that $\vec{g}_o$ is perpendicular to the ray in the object space and $\vec{g}_1$ is perpendicular to the ray in the image space, and both are directed away from the axis (see Figure 1). Let Ox, Oy, Oz be Cartesian rectangular coordinate axes, with origin at the Gaussian focus, with Ox in the direction of $\vec{e}_o$ and with Oz along the axis of the system, pointing away from the plane of the exit pupil into the image space. Finally, let $\vec{i}$, $\vec{j}$ and $\vec{k}$ be unit vectors in the direction of the coordinate axes.

The electric and the magnetic vectors are orthogonal to the ray [see Born and Wolf (1959), § 3.1]. Hence $\vec{e}_1$ lies in the plane of $\vec{g}_1$ and $\vec{g}_1 \wedge \vec{s}$, i.e.

$$\hat{\vec{e}}_1 = \alpha \vec{g}_1 + \beta(\vec{g}_1 \wedge \vec{s}) , \tag{2.14}$$

where α and β are some constants. To determine α and β we make use of a result mentioned earlier, namely that as the light traverses the system, the angle between the electric (and also the magnetic) vector and the meridional plane of the ray remains constant. Moreover, each of these vectors remains on the same side of the meridional plane. These results imply that

$$(2.15)\qquad \begin{cases} \vec{g}_1 \cdot \hat{\vec{e}}_1 = \vec{g}_o \cdot \vec{i} \ , \\ (\vec{g}_1 \wedge s_1) \cdot \hat{e}_1 = (\vec{g}_o \wedge \vec{k}) \cdot \vec{i} \ . \end{cases}$$

On substituting from (2.14) into (2.15) we find that

$$(2.16)\qquad \alpha = \vec{g}_o \cdot \vec{i} \ , \ \beta = (\vec{g}_o \wedge \vec{k}) \cdot \vec{i} = \vec{g}_o \cdot (\vec{k} \wedge \vec{i}) = \vec{g}_o \cdot \vec{j} \ ,$$

and from (2.12), (2.13) and (2.15) it follows that

$$(2.17)\qquad \vec{a} = f \mathcal{L}_o \sqrt{\cos\theta} \left[(\vec{g}_o \cdot \vec{i}) \vec{g}_1 + (\vec{g}_o \cdot \vec{j})(\vec{g}_1 \wedge \vec{s}) \right] .$$

It will now be convenient to introduce spherical polar coordinates r, θ, ϕ ($r > 0$, $0 \leq \theta < \pi$, $0 \leq \phi < 2\pi$), with the polar axis $\theta = 0$ in the z-direction, and with the azimuth $\phi = 0$ containing the electric vector in the object space. The components s_x, s_y, s_z of the unit vector $\vec{s}$ along a ray in the image space and the coordinates (x, y, z) of a point P in the image region may be expressed in the form

$$(2.18a)\qquad s_x = \sin\theta \cos\phi \ , \quad s_y = \sin\theta \sin\phi \ , \quad s_z = \cos\theta \ ,$$

$$(2.18b)\qquad x = r_P \sin\theta_P \cos\phi_P \ , \ y = r_P \sin\theta_P \sin\phi_P \ , \ z = r_P \cos\theta_P \ ,$$

so that the term in the exponent of the integrals (2.1) and (2.3) becomes

$$(2.19)\qquad s_x x + s_y y + s_z z = r_P \cos\epsilon \ ,$$

where

$$(2.20)\qquad \cos\epsilon = \cos\theta \cos\theta_P + \sin\theta \sin\theta_P \cos(\phi - \phi_P) \ .$$

Let (θ_o, ϕ_o) and (θ_1, ϕ_1) be the polar angles of $\vec{g}_o$ and $\vec{g}_1$ respectively. Then evidently (see Figure 1)

$$(2.21) \qquad \phi_o = \phi_1 = \phi - \pi \ , \ \theta_o = \frac{\pi}{2} \ , \ \theta_1 = \frac{\pi}{2} - \theta \ ,$$

so that

$$(2.22) \qquad \begin{cases} \vec{g}_o = - \cos\phi \ \vec{i} - \sin\phi \ \vec{j} \ , \\ \vec{g}_1 = - \cos\theta\cos\phi \ \vec{i} - \cos\theta\sin\phi \ \vec{j} + \sin\theta \ \vec{k} \ . \end{cases}$$

It follows on substitution from (2.22) and (2.18a) into (2.17) and (2.6) that the Cartesian components of the strength vectors $\vec{a}$ and $\vec{b}$ are

$$(2.23) \qquad \begin{cases} a_x = f\ell_o\sqrt{\cos\theta}\left[\cos\theta + \sin^2\phi(1 - \cos\theta)\right] \ , \\ a_y = f\ell_o\sqrt{\cos\theta}\left[(\cos\theta - 1)\cos\phi\sin\phi\right] \ , \\ a_z = -f\ell_o\sqrt{\cos\theta}\sin\theta\cos\phi \ , \end{cases}$$

$$(2.24) \qquad \begin{cases} b_x = f\ell_o\sqrt{\cos\theta}\left[(\cos\theta - 1)\cos\phi\sin\phi\right] \ , \\ b_y = f\ell_o\sqrt{\cos\theta}\left[1 - \sin^2\phi(1 - \cos\theta)\right] \ , \\ b_z = -f\ell_o\sqrt{\cos\theta}\sin\theta\sin\phi \ . \end{cases}$$

Finally, we also need an expression, in terms of θ and ϕ, for the quantity $ds_x \, ds_y/s_z$. which enters our basic diffraction integrals (2.2) and (2.3). According to equation (2.6) of the previous report, this quantity represents the element $d\Omega$ of the solid angle and is given by

$$(2.25) \qquad \frac{ds_x ds_y}{s_z} = d\Omega = \sin\theta d\theta d\phi \ .$$

On substituting from (2.23), (2.24), (2.25), (2.11) and (2.7) into (2.2) and (2.3) we obtain the following expressions for the Cartesian components $\vec{e}$ and $\vec{h}$:

$$(2.26)\quad \begin{cases} e_x = -\dfrac{iA}{\pi}\displaystyle\int_0^{\alpha}\int_0^{2\pi} \sqrt{\cos\theta}\sin\theta \left\{\cos\theta + (1-\cos\theta)\sin^2\phi\right\} \exp\left[ikr_p\cos\epsilon\right] d\theta d\phi \ , \\ e_y = \dfrac{iA}{\pi}\displaystyle\int_0^{\alpha}\int_0^{2\pi} \sqrt{\cos\theta}\sin\theta(1-\cos\theta)\cos\phi\sin\phi\exp\left[ikr_p\cos\epsilon\right] d\theta d\phi \ , \\ e_z = \dfrac{iA}{\pi}\displaystyle\int_0^{\alpha}\int_0^{2\pi} \sqrt{\cos\theta}\sin^2\theta\cos\phi\exp\left[ikr_p\cos\epsilon\right] d\theta d\phi \ ; \end{cases}$$

$$(2.27)\quad \begin{cases} h_x = \dfrac{iA}{\pi}\displaystyle\int_0^{\alpha}\int_0^{2\pi} \sqrt{\cos\theta}\sin\theta(1-\cos\theta)\cos\phi\sin\phi\exp\left[ikr_p\cos\epsilon\right] d\theta d\phi \ , \\ h_y = -\dfrac{iA}{\pi}\displaystyle\int_0^{\alpha}\int_0^{2\pi} \sqrt{\cos\theta}\sin\theta \left\{1-(1-\cos\theta)\sin^2\phi\right\} \exp\left[ikr_p\cos\epsilon\right] d\theta d\phi \ , \\ h_z = \dfrac{iA}{\pi}\displaystyle\int_0^{\alpha}\int_0^{2\pi} \sqrt{\cos\theta}\sin^2\theta\sin\phi\exp\left[ikr_p\cos\epsilon\right] d\theta d\phi \ . \end{cases}$$

Here $\cos\epsilon$ is given by (2.19), α is the angular semi-aperture on the image side, i.e. 2α is the angle which the diameter of the exit pupil subtends at the geometrical focus and A is the constant

$$(2.28)\qquad A = kf\ell_o / 2 = \pi f\ell_o / \lambda \ .$$

The integration with respect to ϕ can immediately be carried out with the help of the following formulas* which are valid for any integral value of n :

$$(2.29)\quad \begin{cases} \int_0^{2\pi} \cos n\phi \exp\left[i\rho\cos(\phi-\gamma)\right]d\phi = 2\pi i^n J_n(\rho)\cos n\gamma , \\ \int_0^{2\pi} \sin n\phi \exp\left[i\rho\cos(\phi-\gamma)\right]d\phi = 2\pi i^n J_n(\rho)\sin n\gamma . \end{cases}$$

Here $J_n(\rho)$ is the Bessel function of the first kind and order n. If in (2.26) and (2.27) we use the identities $\cos\phi\sin\phi = \frac{1}{2}\sin 2\phi$, $\sin^2\phi = \frac{1}{2}(1-\cos 2\phi)$ and apply (2.29) we finally obtain the following expressions for the components of the field vectors at a point P in the image region:

---

*These formulas may be derived as follows: We start from the integral representation of J_n:

$$\int_0^{2\pi} e^{i(n\phi+\rho\cos\phi)}d\phi = 2\pi i^n J_n(\rho)$$

(cf. Watson (1952), p. 20 (5)). We change ϕ into $\phi-\gamma$ and multiply both sides of (2.30) by $e^{in\gamma}$ and express the resulting formula as follows:

$$\int_0^{2\pi} \cos n\phi\, e^{i\rho\cos(\phi-\gamma)}d\phi + i\int_0^{2\pi} \sin n\phi\, e^{i\rho\cos(\phi-\gamma)}d\phi = 2\pi i^n J_n(\rho)\left[\cos n\gamma + i\sin n\gamma\right] .$$

Each side consists of two terms, one of which is an even function of γ and the other an odd function of γ. This is only possible if the even terms are equal to each other and so are the odd terms, and this implies (2.29).

$$(2.30)\quad \begin{cases} e_x(P) = -\,iA\,(I_o + I_2 \cos 2\phi_P)\,, \\ e_y(P) = -\,iA\,I_2 \sin 2\phi_P\,, \\ e_z(P) = -\,2A\,I_1 \cos \phi_P\,, \end{cases}$$

$$(2.31)\quad \begin{cases} h_x(P) = -\,iA\,I_2 \sin 2\phi_P\,, \\ h_y(P) = -\,iA\,(I_o - I_2 \cos 2\phi_P)\,, \\ h_z(P) = -\,2A\,I_1 \sin \phi_P\,, \end{cases}$$

where

$$(2.32)\quad \begin{cases} I_o = I_o(kr_P,\theta_P,\alpha) = \displaystyle\int_o^\alpha \sqrt{\cos\theta}\,\sin\theta\,(1+\cos\theta)\,J_o(kr_P \sin\theta \sin\theta_P) \\ \qquad\qquad \cdot \exp\left[ikr_P \cos\theta \cos\theta_P\right] d\theta\,, \\ I_1 = I_1(kr_P,\theta_P,\alpha) = \displaystyle\int_o^\alpha \sqrt{\cos\theta}\,\sin^2\theta\,J_1(kr_P \sin\theta \sin\theta_P) \\ \qquad\qquad \cdot \exp\left[ikr_P \cos\theta \cos\theta_P\right] d\theta\,, \\ I_2 = I_2(kr_P,\theta_P,\alpha) = \displaystyle\int_o^\alpha \sqrt{\cos\theta}\,\sin\theta\,(1-\cos\theta)\,J_2(kr_P \sin\theta \sin\theta_P) \\ \qquad\qquad \cdot \exp\left[ikr_P \cos\theta \cos\theta_P\right] d\theta\,. \end{cases}$$

The formulas (2.30) and (2.31) represent the analytic solution of our problem. They express the field at any point P (spherical polar coordinates r_P, θ_P, ϕ_P) in terms of the three integrals I_0, I_1 and I_2. We shall now discuss some consequences of these formulas.

3. The image field

It is convenient at this stage to introduce certain 'optical coordinates', which are a natural generalization of the coordinates (defined by (3.1a) below) employed frequently in connection with diffraction in systems with low angular aperture. We define these optical coordinates by the formulas*

$$(3.1)\quad \begin{cases} u = kr_P \cos\Theta_P \sin^2\alpha = kz \sin^2\alpha , \\ v = kr_P \sin\Theta_P \sin\alpha = k\sqrt{x^2 + y^2}\ \sin\alpha . \end{cases}$$

From now on we shall omit the subscript P in the symbol ϕ_P for the azimuthal angle, and specify the point P of observation by the three parameters, u, v and ϕ ($u \gtrless 0$, $v \geq 0$, $0 \leq \phi < 2\pi$). The geometrical focal plane is given by $u = 0$, the axis by $v = 0$ and the edge of the geometrical shadow $\left(\sqrt{x^2 + y^2} = \pm z \tan\alpha\right)$ by $v = \pm u \sec\alpha$.

The integrals (2.32) are now regarded as functions of u and v,

$$(3.2)\quad \begin{cases} I_0(u,v) = \displaystyle\int_0^\alpha \sqrt{\cos\Theta}\,\sin\Theta\,(1+\cos\Theta)\,J_0\!\left(\frac{v\sin\Theta}{\sin\alpha}\right)\exp\left[\frac{iu\cos\Theta}{\sin^2\alpha}\right]d\Theta , \\ I_1(u,v) = \displaystyle\int_0^\alpha \sqrt{\cos\Theta}\,\sin^2\Theta\,J_1\!\left(\frac{v\sin\Theta}{\sin\alpha}\right)\exp\left[\frac{iu\cos\Theta}{\sin^2\alpha}\right]d\Theta , \\ I_2(u,v) = \displaystyle\int_0^\alpha \sqrt{\cos\Theta}\,\sin\Theta\,(1-\cos\Theta)\,J_2\!\left(\frac{v\sin\Theta}{\sin\alpha}\right)\exp\left[\frac{iu\cos\Theta}{\sin^2\alpha}\right]d\Theta . \end{cases}$$

---

*When the angular aperture is small ($\alpha \ll 1$), the formulas (3.1) reduce to

$$(3.1a)\quad \begin{cases} u \sim k\,(\,a/R\,)^2\,z , \\ v \sim k\,(\,a/R\,)\,\sqrt{x^2 + y^2} , \end{cases}$$

where $\sin\alpha \sim \tan\alpha = a/R$, a being the radius of the exit pupil and R the distance between the exit pupil and the focal plane.

We note that

$$(3.3) \qquad I_n(-u,v) = I_n^*(u,v) \quad , \quad (n = 0,1,2) \ ,$$

where the asterisk denotes the complex conjugate. From (2.30), (2.31) and (3.3) we note the following relations which exist between the components of the field vectors at any two points $P_1(u,v,\phi)$ and $P_2(-u,v,\phi)$, which are symmetrically placed with respect to the focal plane:

$$(3.4) \quad \begin{cases} e_x(-u,v,\phi) = -e_x^*(u,v,\phi) \ , & h_x(-u,v,\phi) = -h_x^*(u,v,\phi) \ , \\ e_y(-u,v,\phi) = -e_y^*(u,v,\phi) \ , & h_y(-u,v,\phi) = -h_y^*(u,v,\phi) \ , \\ e_z(-u,v,\phi) = e_z^*(u,v,\phi) \ , & h_z(-u,v,\phi) = h_z^*(u,v,\phi) \ , \end{cases}$$

If $|e_x|$ denotes the amplitude and Ψ_x the phase of e_x, the first relation in (3.4) implies that*

$$(3.5a) \qquad |e_x(-u,v,\phi)| = |e_x(u,v,\phi)| \ ,$$

and

$$(3.5b) \qquad \Psi_x(-u,v,\phi) = -\Psi_x(u,v,\phi) + \pi \pmod{2\pi} \ .$$

The relation (3.5a) shows that for any two points which are symmetrically situated with respect to the focal plane, the amplitude of the e_x's are

---

*The quantity mod 2π on the right of an equation denotes that the two sides of the equation are indeterminate to the extent of an additive constant $2m\pi$ where m is any integer.

the same, and (3.5b) shows that there exists also a simple relation between the phases. The appearance of the additive factor π on the right of (3.5b) is connected with the well-known phase anomaly at focus [cf Born and Wolf, (1959), § 8.8, eq. (43)]. From (3.4) we see that relations of the form (3.5a) holds also for all the other components. However, relation of the form (3.5b) holds for the phases of e_x, e_y, h_x and h_y only. For the phase of the remaining two components we have, in place of (3.5b), relations of the following form:

$$\Psi_z(-u,v,\phi) = -\Psi_z(u,v,\phi) \quad (\text{mod } 2\pi). \tag{3.5c}$$

Thus the components of $\vec{e}$ and $\vec{h}$ in the direction of the axis of revolution of the system have no phase anomaly.

From (2.30) and (2.31) it is also seen that

$$\begin{cases} h_x(u,v,\phi) = -e_y(u,v,\phi - \frac{\pi}{2}), \\ h_y(u,v,\phi) = e_x(u,v,\phi - \frac{\pi}{2}), \\ h_z(u,v,\phi) = e_z(u,v,\phi - \frac{\pi}{2}). \end{cases} \tag{3.6}$$

Hence in any fixed plane of observation (u = constant), the $\vec{e}$ and $\vec{h}$ fields are the same but are rotated with respect to each other by 90° around the z-axis; this, of course, might have been expected, since the $\vec{e}$ and $\vec{h}$ fields in the object space have this relationship, and the laws relating to the transmission of these fields through the system are the same.

3.1 Polarization of the image field

To examine the state of polarization of the image field, we separate the real and imaginary parts of the integrals (3.2) and write

$$(3.7) \qquad I_n(u,v) = I_n^{(r)}(u,v) + iI_n^{(i)}(u,v) , \quad (n = 0,1,2)$$

where $I_n^{(r)}$ and $I_n^{(i)}$ are real. We also write

$$(3.8) \qquad \vec{e}(u,v,\phi) = \vec{p}(u,v,\phi) + i\vec{q}(u,v,\phi) ,$$

where $\vec{p}$ and $\vec{q}$ are real vectors; they are a pair of conjugate semi-diameters of the polarization ellipse of the electric vector. According to (2.30), (3.7) and (3.8)

$$(3.9) \quad \begin{cases} p_x(u,v,\phi) = A(I_o^{(i)} + I_2^{(i)}\cos 2\phi) , & q_x(u,v,\phi) = -A(I_o^{(r)} + I_2^{(r)}\cos 2\phi), \\ p_y(u,v,\phi) = A\, I_2^{(i)} \sin 2\phi , & q_y(u,v,\phi) = -A\, I_2^{(r)} \sin 2\phi , \\ P_z(u,v,\phi) = -2A\, I_1^{(r)} \cos\phi , & q_z(u,v,\phi) = -2A\, I_1^{(i)} \cos\phi . \end{cases}$$

Since, according to (3.4) the integrals I_o, I_1 and I_2 are all real when u = 0 (focal plane), it follows that

$$(3.10) \quad \begin{cases} p_x(o,v,\phi) = 0 , & q_x(o,v,\phi) = -A[I_o(o,v) + I_2(o,v)\cos 2\phi] , \\ p_y(o,v,\phi) = 0 , & q_y(o,v,\phi) = -A\, I_2(o,v) \sin 2\phi , \\ p_z(o,v,\phi) = -2A\, I_1(o,v) \cos\phi , & q_z(o,v,\phi) = 0 . \end{cases}$$

From (3.10) we see that in the focal plane $\vec{p}.\vec{q} = 0$, i.e. the conjugate semi-diameters are at right angles to each other; hence in the focal plane, $\vec{p}$ and $\vec{q}$ are the semi-axes of the polarization ellipse of the electric vector. Moreover, the $\vec{p}$-axis is perpendicular to the focal plane and the $\vec{q}$-axis lies in the focal plane. Thus, the polarization ellipse of the electric vector at any point in the focal plane is at right angles to the focal plane. The angle $\chi(v,\phi)(-\pi/2 < \chi \leq \pi/2)$ between the plane of the polarization ellipse and the plane $\phi = 0$ (the xz-plane) is given by

$$(3.11) \qquad \tan \chi\,(v,o) = \frac{q_y(o,v,\phi)}{q_x(o,v,\phi)} = \frac{I_2(o,v)\,\sin 2\phi}{I_o(o,v) + I_2(o,v)\,\cos 2\phi}\ ,$$

and the two axes of the polarization ellipse are in the ratio

$$(3.12) \qquad \rho\,(v,\phi) = \frac{|p_z\,(o,v,\phi)|}{+\sqrt{q_x^2(o,v,\phi) + q_y^2(o,v,\phi)}}$$

$$= \frac{2|I_1(o,v)\,\cos\phi|}{+\sqrt{I_o^2(o,v) + I_2^2(o,v) + 2I_o(o,v)I_2(o,v)\cos 2\phi}}\ .$$

Along the y-axis ($\phi = \frac{\pi}{2}$ or $\frac{3\pi}{2}$) only one of the components in (3.10), namely q_x, is different from zero. Hence at each point of the y-axis and, in particular, at the focus itself, the electric field is linearly polarized in the x-direction, i.e., in the direction of vibrations of the electric field in the object space. Since $\vec{p}$ also vanishes when $I_1(o,v) = 0$, the electric field is also linearly polarized along circles centered on the focus, whose radii (measured in v-units) are given by the roots of this equation; however, along these circles, the direction of vibrations is not in general in the x-direction.

The behavior of χ and ρ in the focal plane of an aplanatic system of angular semi-aperture $\alpha = 60^{\circ}$ is shown in Figure 2. The figure was computed from the formulas (3.11), (3.12) and (3.2) by means of the Manchester University Electronic Computor Mark I. The details of these and other computations relating to this paper are given in a thesis by one of the authors (Richards, 1956b).

Figure 2(a) shows that in the central nucleus of the image $\chi \sim 0^{\circ}$, i.e. in this region the electric vector vibrates in planes nearly parallel to the plane which contains the direction of the electric vibrations in the object space and the axis of the system. According to Figure 2(b) the axial component (e_z) is not negligible in all parts of the central nucleus.

The state of polarization of the field at points on the axis of the system ($v = 0$) is also of interest. Since $I_1(u,0) = I_2(u,0) = 0$ for all values of u, it follows from (2.30) that on the axis $e_y = e_z = 0$. Hence the electric vector at each point on the axis of revolution in the image space is linearly polarized, and its direction is the same as the direction of the electric vector in the object space.

3.2 The energy density

Let

$$
(3.13)\quad \begin{cases} \langle w_e(u,v,\phi)\rangle = \frac{1}{8\pi}\langle \vec{E}^2\rangle = \frac{1}{16\pi}(\vec{e}\,.\,\vec{e}^{\,*}), \\ \langle w_m(u,v,\phi)\rangle = \frac{1}{8\pi}\langle \vec{H}^2\rangle = \frac{1}{16\pi}(\vec{h}\,.\,\vec{h}^{\,*}), \\ \langle w\,(u,v,\phi)\rangle = \langle w_e(u,v,\phi)\rangle + \langle w_m(u,v,\phi)\rangle \\ \qquad\qquad = \frac{1}{16\pi}(\vec{e}\,.\,\vec{e}^{\,*} + \vec{h}\,.\,\vec{h}^{\,*}), \end{cases}
$$

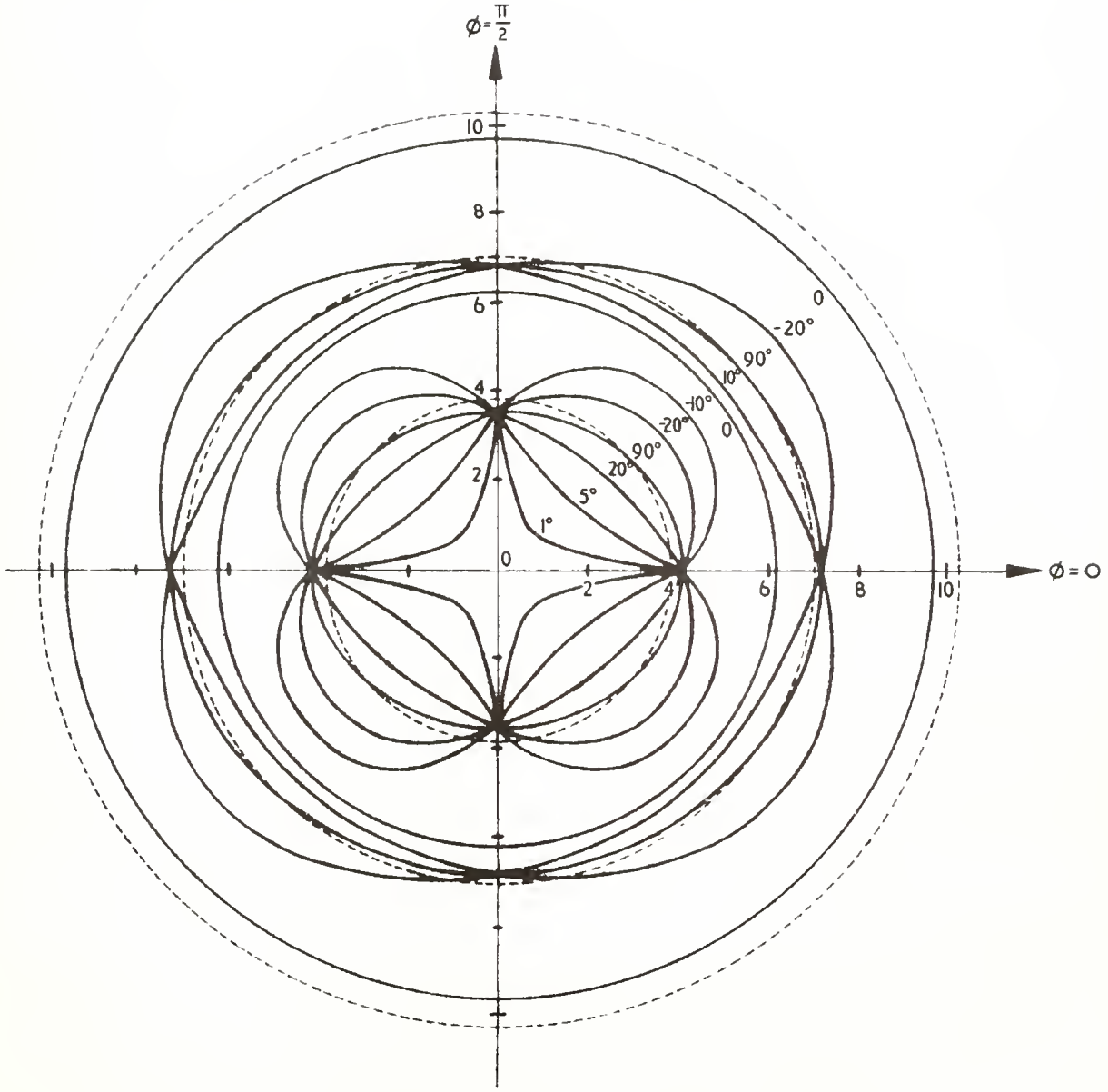

FIGURE 2(a)

For captions to Figures see page 40.

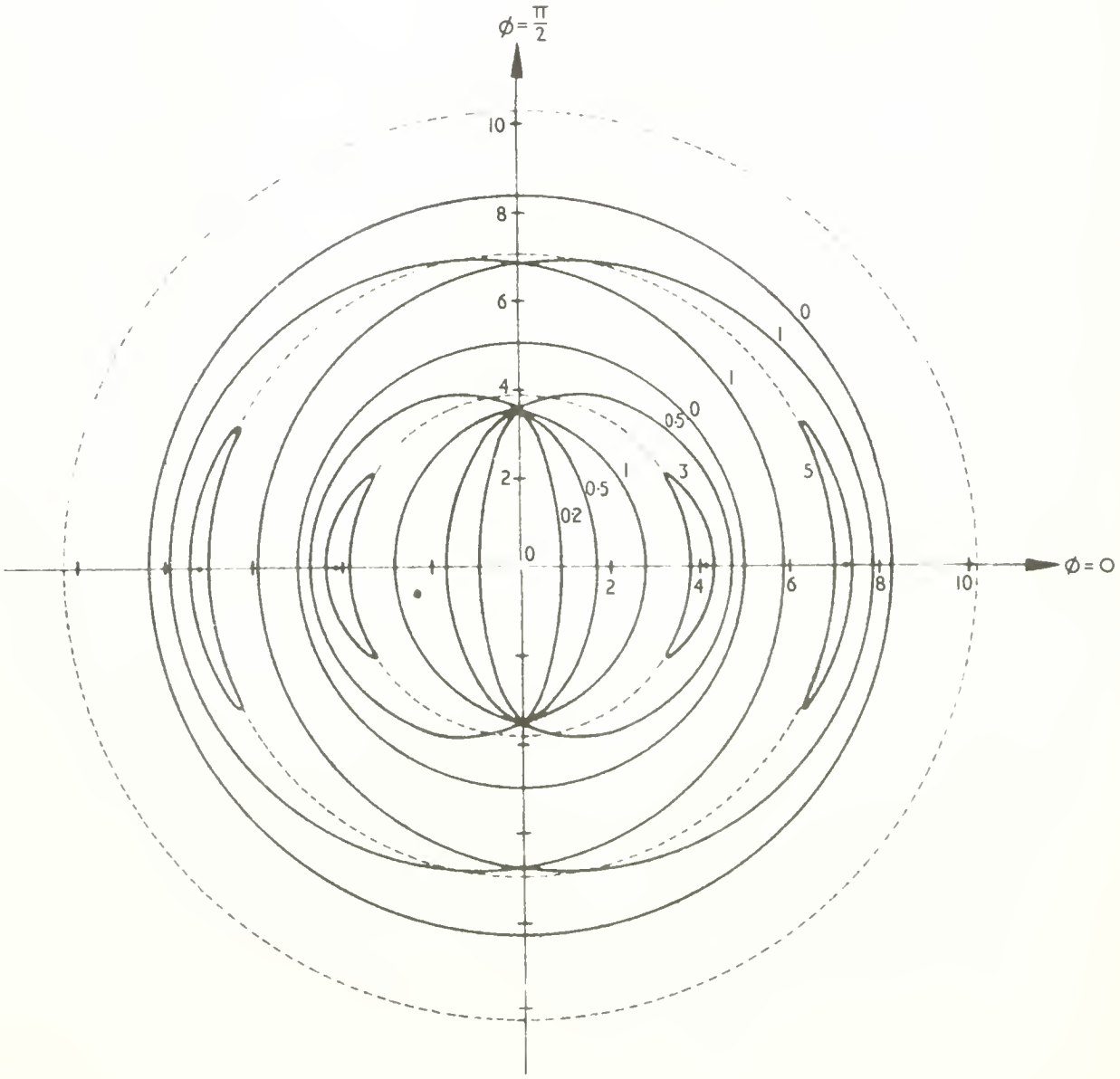

FIGURE 2(b)

denote the electric energy density, the magnetic energy density and the total energy density, each averaged over a time interval which is large compared to the basic period $T = 2\pi/\omega$. From (2.30) and (3.13), we have

$$(3.14)\quad \begin{cases} \langle w_e(u,v,\phi)\rangle = \dfrac{A^2}{16\pi}\left\{|I_o|^2 + 4|I_1|^2\cos^2\phi + |I_2|^2 + 2\cos 2\phi\,\mathcal{R}(I_o I_2^*)\right\}, \\ \langle w_m(u,v,\phi)\rangle = \dfrac{A^2}{16\pi}\left\{|I_o|^2 + 4|I_1|^2\sin^2\phi + |I_2|^2 - 2\cos 2\phi\,\mathcal{R}(I_o I_2^*)\right\}, \\ \langle w(u,v,\phi)\rangle = \dfrac{A^2}{8\pi}\left\{|I_o|^2 + 2|I_1|^2 + |I_2|^2\right\}, \end{cases}$$

where $\mathcal{R}$ denotes the real part.

We note that because of (3.3) [as, of course, is also evident from (3.4)]

$$(3.15)\quad \langle w_e(-u,v,\phi)\rangle = \langle w_e(u,v,\phi)\rangle ,$$

with similar relations involving $\langle w_m\rangle$ and $\langle w\rangle$. Hence <u>the distributions of the time averaged electric energy density, magnetic energy density and total energy density are symmetrical about the focal plane u = 0</u>.

Further we see that

$$(3.16)\quad \langle w_m(u,v,\phi)\rangle = \langle w_e(u,v,\phi - \tfrac{\pi}{2})\rangle .$$

Thus <u>the distribution of the time averaged magnetic energy density is identical with the distribution of the time averaged electric energy density, but the distributions are rotated with respect to each other by 90° about the axis of the system</u>. We also note that $\langle w\rangle$ is independent of ϕ, so that

the loci of constant time averaged total energy density are surfaces of revolution about the axis of revolution of the system.

Since for all u $I_1(u,0) = I_2(u,0) = 0$, we see from (3.14) that along the axis of revolution in the image space*

$$(3.17) \qquad \langle w_e \rangle = \langle w_m \rangle = \frac{1}{2} \langle w \rangle = \frac{A^2}{16\pi} |I_o(u,0)|^2.$$

When $u = v = 0$, we have from (3.2)

$$(3.18) \qquad I_o(0,0) = \int_0^\alpha \sqrt{\cos\theta}\, \sin\theta\, (1 + \cos\theta)\, d\theta$$

$$= \frac{16}{15} \left\{ 1 - \frac{5}{8} \cos^{(3/2)}\alpha\, (1 + \frac{3}{5} \cos\alpha) \right\},$$

so that at the focus itself

$$(3.19) \qquad \langle w_e \rangle = \langle w_m \rangle = \frac{1}{2}\langle w \rangle = \frac{A^2}{15\pi} \left\{ 1 - \frac{5}{8} \cos^{(3/2)}\alpha (1 + \frac{3}{5} \cos\alpha) \right\}.$$

In Figure 3 contours, computed from (3.14), of the time averaged electric energy density in the focal planes of aplanatic systems of selected angular semi-apertures α are shown. The contours of the time averaged magnetic energy density are, according to (3.16), identical with those for the time averaged electric energy, but are rotated by 90° about the normal to the plane of the figure.

---

*Curves which illustrate the behavior of these quantities along the axis of revolution are given in Richards (1956a), 358. The paper also contains curves which give the ratio (as function of α) between the values at focus computed from (3.19) and those computed by the application of the Huygens-Kirchhoff scalar diffraction theory.

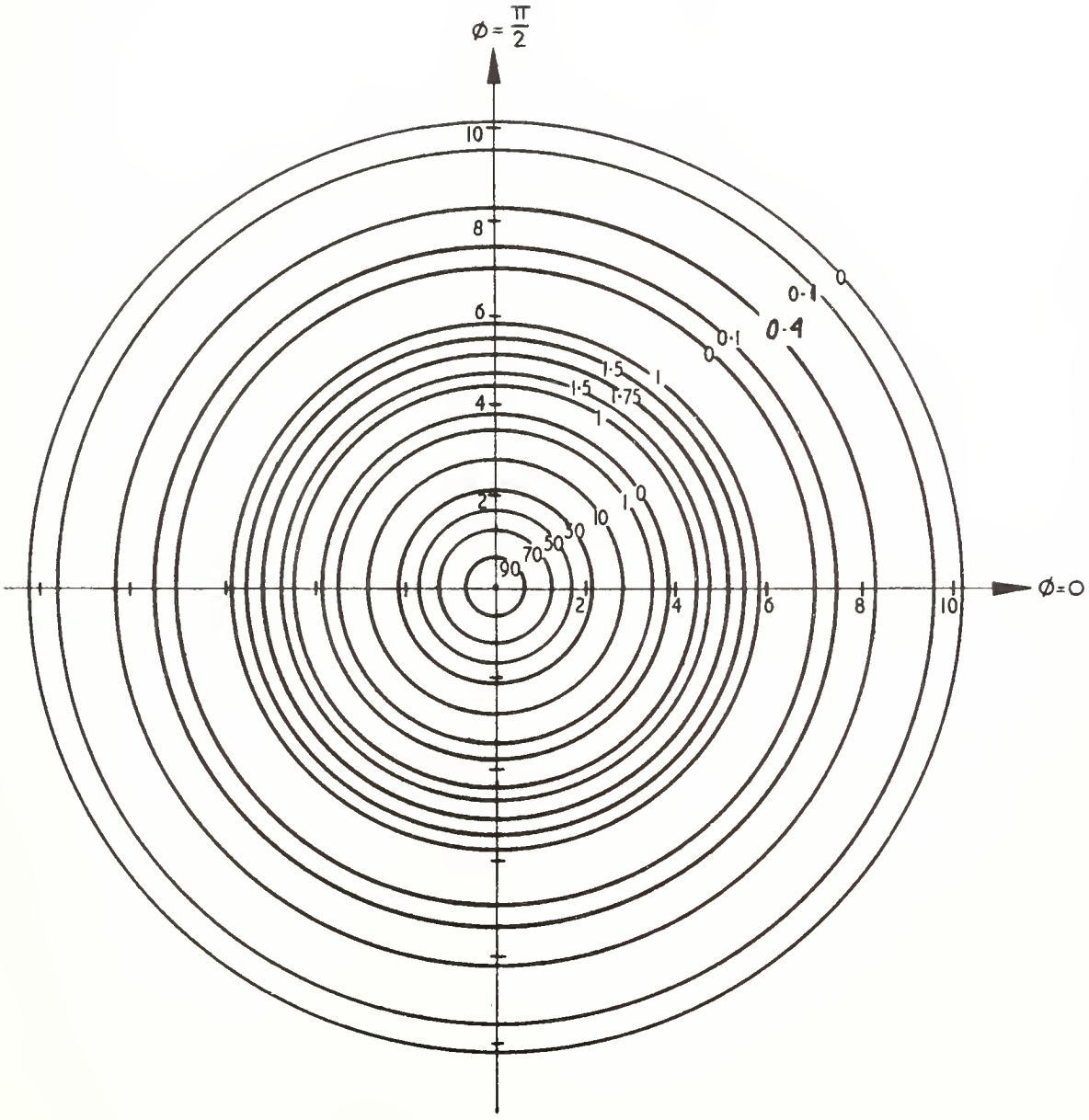

FIGURE 3(a)

For captions to Figures see page 40.

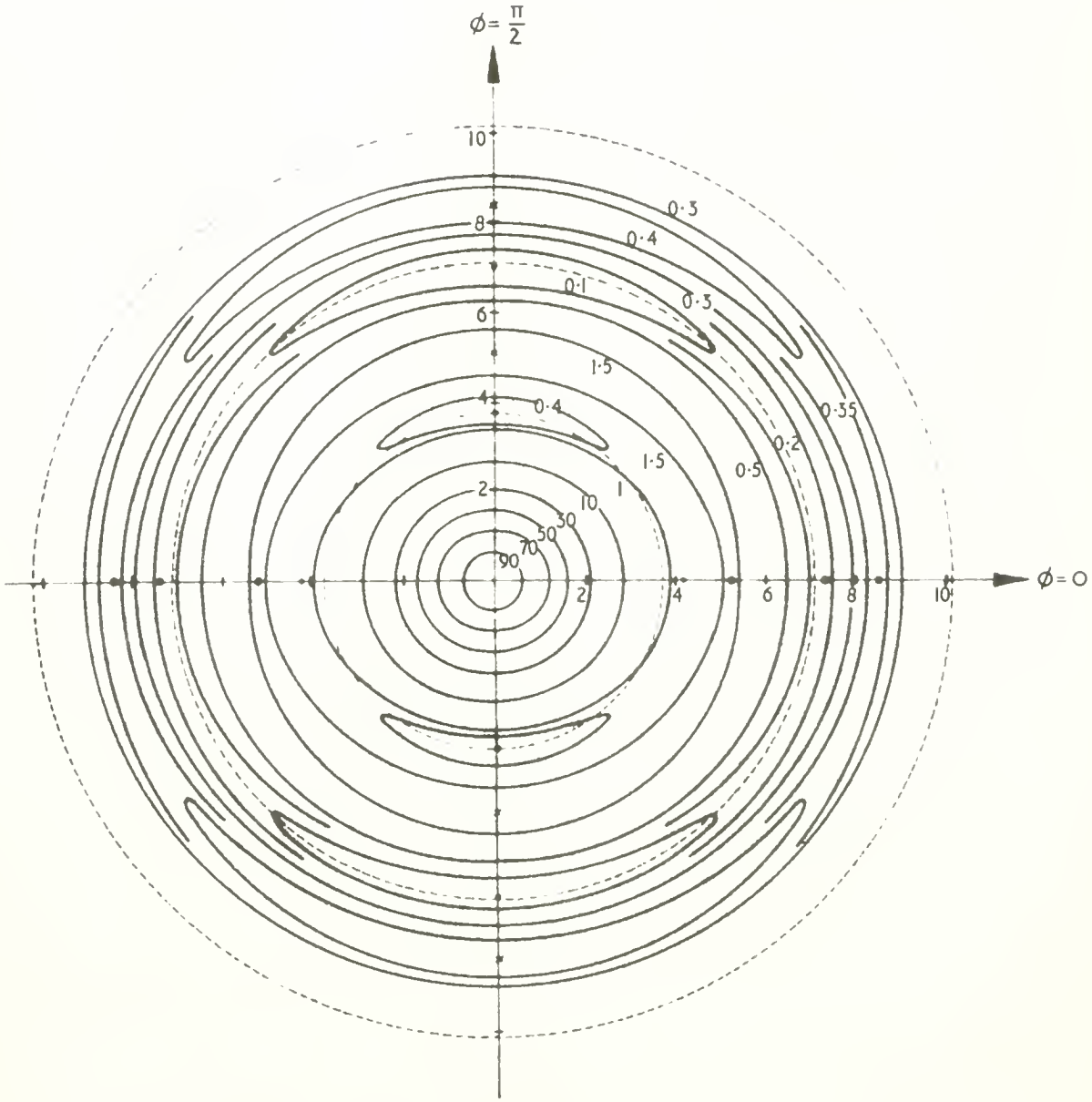
$\phi = \frac{\pi}{2}$
$\phi = 0$
10
8
6
4
2
0·3
0·4
0·1
0·3
1·5
0·4
0·35
0·2
1·5
0·5
1
10
30
50
70
90
2
4
6
8
10

FIGURE 3(b)

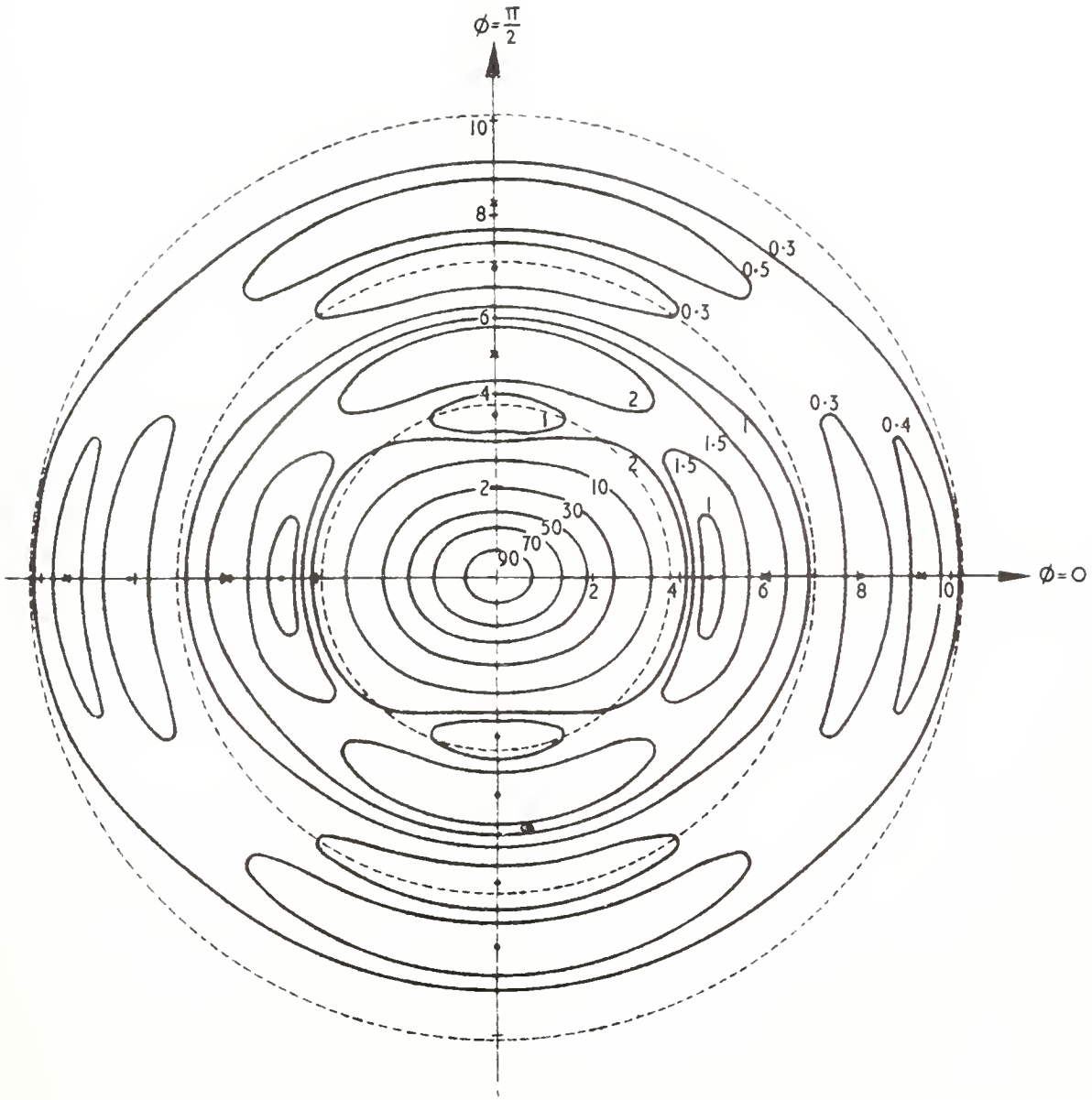
$\phi=\frac{\pi}{2}$
$\phi=0$
10
8
6
4
2
0·3
0·5
0·3
2
1
1·5
1
0·3
0·4
2
1·5
2
10
30
50
70
90
1
2
4
6
8
10

FIGURE 3(c)

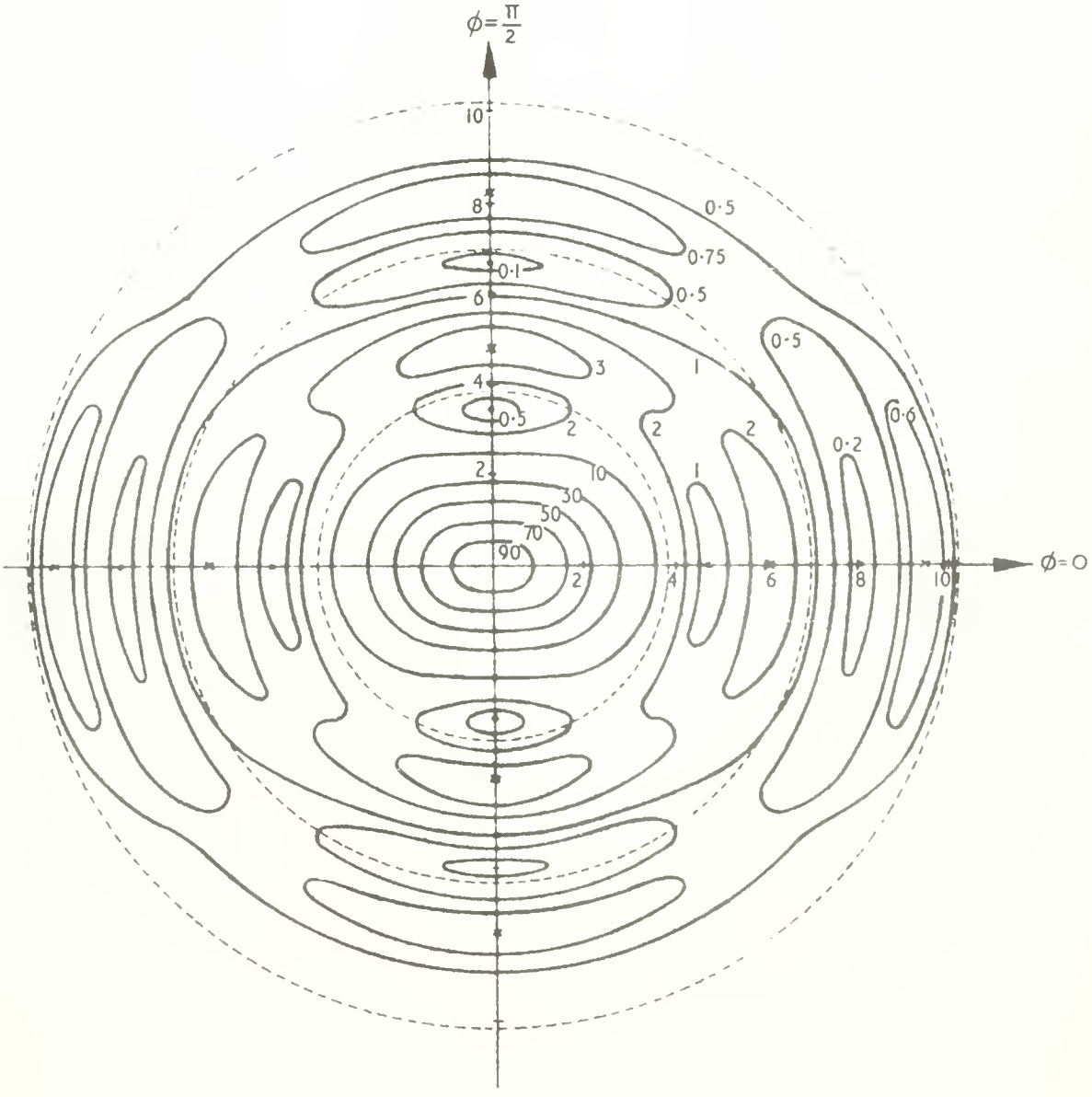
$\phi=\frac{\pi}{2}$
$\phi=0$
10
8
6
4
2
0·5
0·75
0·1
0·5
3
1
0·5
0·6
0·2
2
10
30
50
70
90
2
4
6
8
10

FIGURE 3 (d)

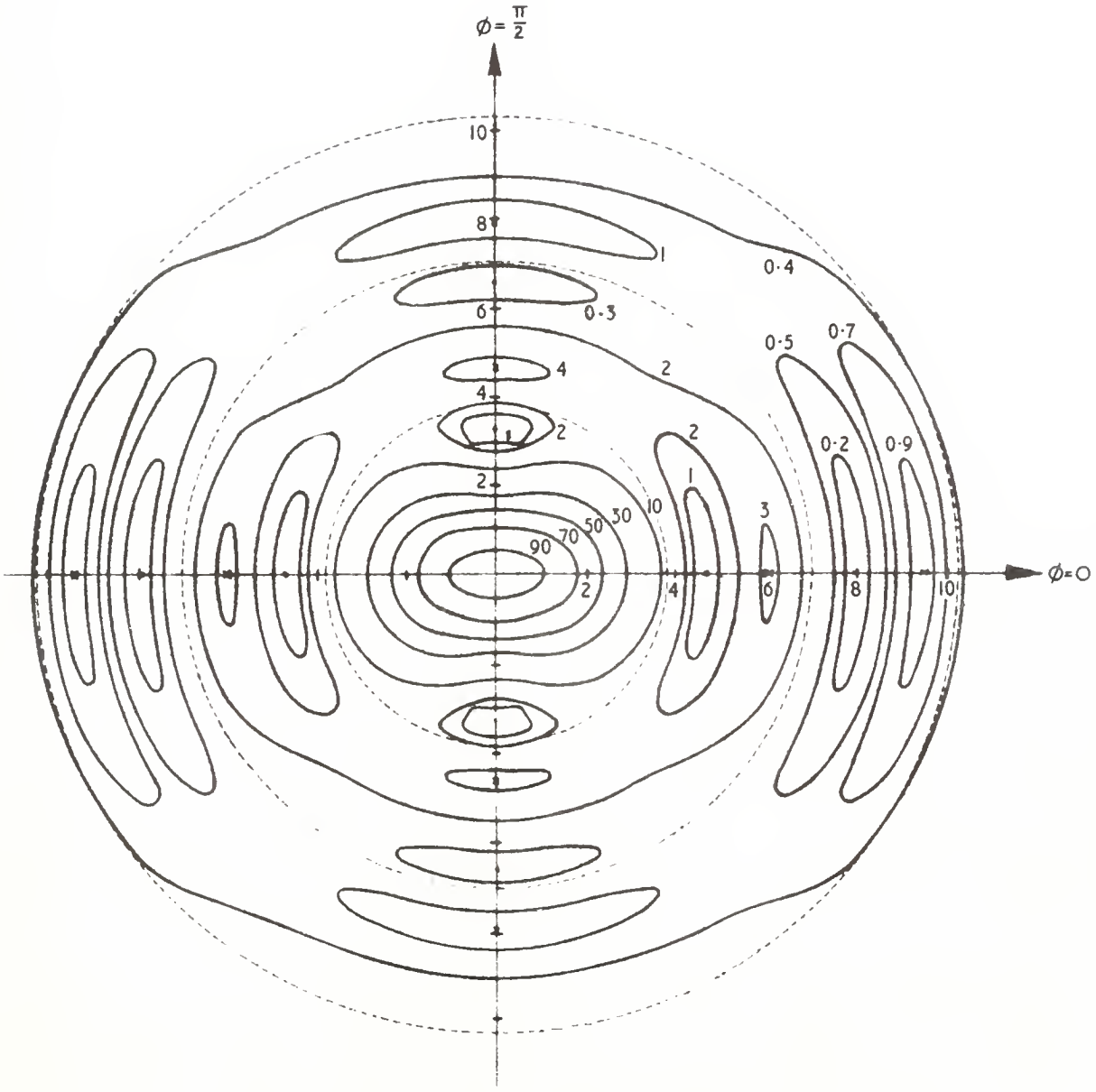
$\phi = \frac{\pi}{2}$
10
8
6
4
2
1
0·4
0·3
0·5
0·7
2
4
2
2
0·2
0·9
2
1
10
3
30
50
70
90
2
4
6
8
10
$\phi = 0$

FIGURE 3(e)

The first diagram in Figure 3 represents the limiting case $\alpha \to 0$. We shall see later (§ 4) that in this case our solution reduces to that obtained on the basis of the usual scalar diffraction theory. Thus 4(a) is the ordinary Airy diffraction pattern: the contours are circles, the first zero contour being given by $v = 1.22\pi = 3.83$. As α increases, the pattern is seen to lose its rotational symmetry; the contours in the neighbourhood of the focus are then approximately elliptical, with their major axes in the direction of the electric vector in the object space ($\phi = 0$). Further away from the center the contours are of a more complicated form and closed loops appear around certain points in the azimuths $\phi = 0, \pi/2, \pi, 3\pi/2$. For large values of α, the ellipticity of the contours becomes quite pronounced and the first minimum in the azimuth $\phi = 0$ is well outside the first zero of the Airy pattern, while in the azimuth $\phi = \pi/2$ it is well inside. Hence, if the wave in the object space is linearly polarized and detectors of electric energy (e.g. a photographic plate) are used, our solution predicts an increase in the resolving power in wide aperture systems for measurements in the azimuth at right angles to that of the electric vector of the incident wave. This conclusion is in agreement with a prediction of Hopkins (1943, 1945) and appears to be supported by early experiments recorded by Carpenter (1901).

The behavior of the time averaged electric energy density along the azimuths $\phi = 0$ and $\phi = \pi/2$ in the focal plane is shown in detail in Figure 4. It is seen that along the azimuth $\phi = 0$, the minima are not true zeros; the minima are, however, zeros along the azimuth $\phi = \pi/2$. The behavior of the time averaged total energy density, which, as already noted, is independent of the azimuth, is also shown in Figures 4.

3.3 The energy flow (Poynting vector)

The time averaged Poynting vector is given by

$$\langle \vec{S} \rangle = \frac{c}{4\pi} \langle \vec{E} \wedge \vec{H} \rangle = \frac{c}{8\pi} \mathcal{R} (\vec{e} \wedge \vec{h}^{\,*}) \,. \tag{3.20}$$

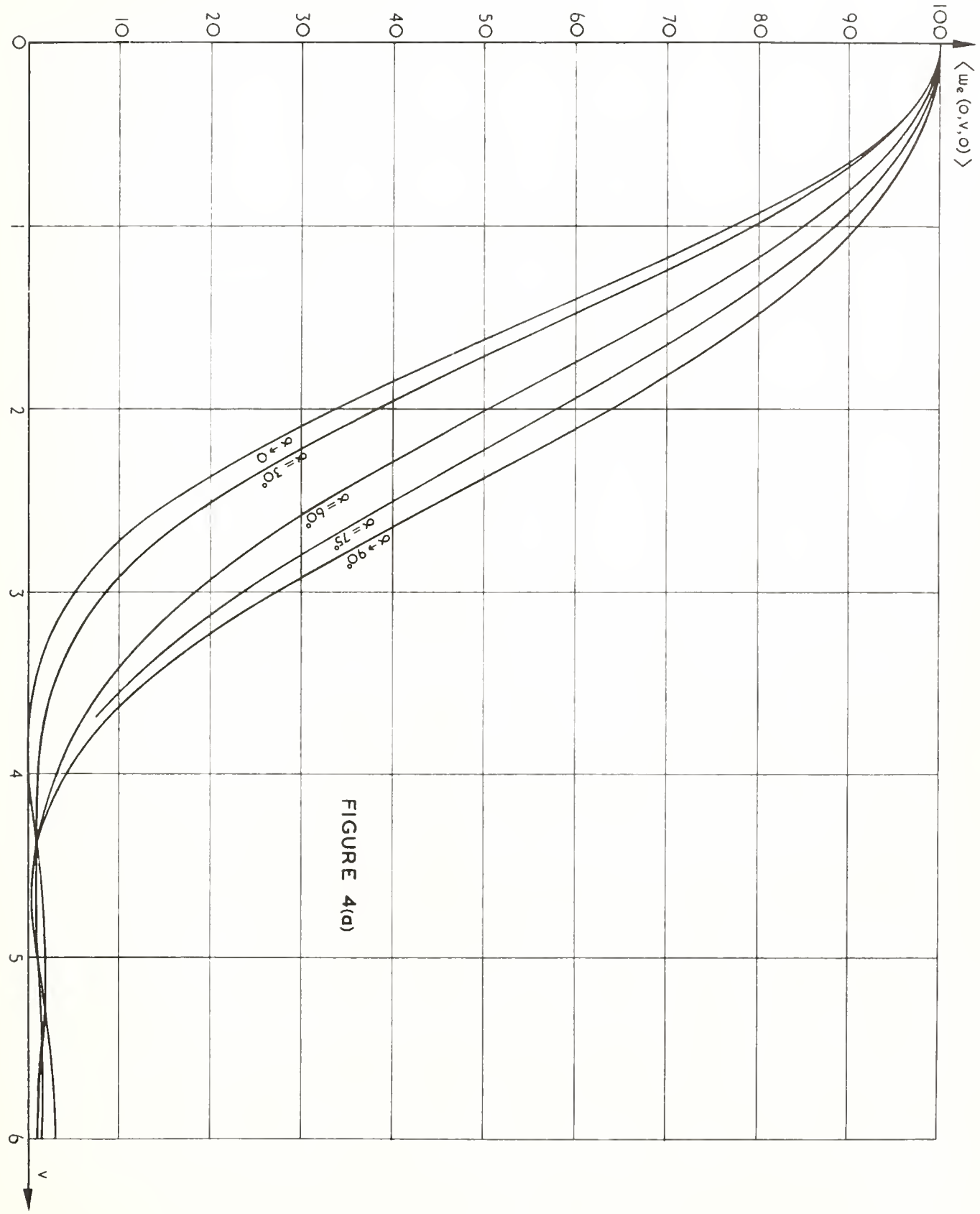

FIGURE 4(a)

For captions to Figures see page 41.

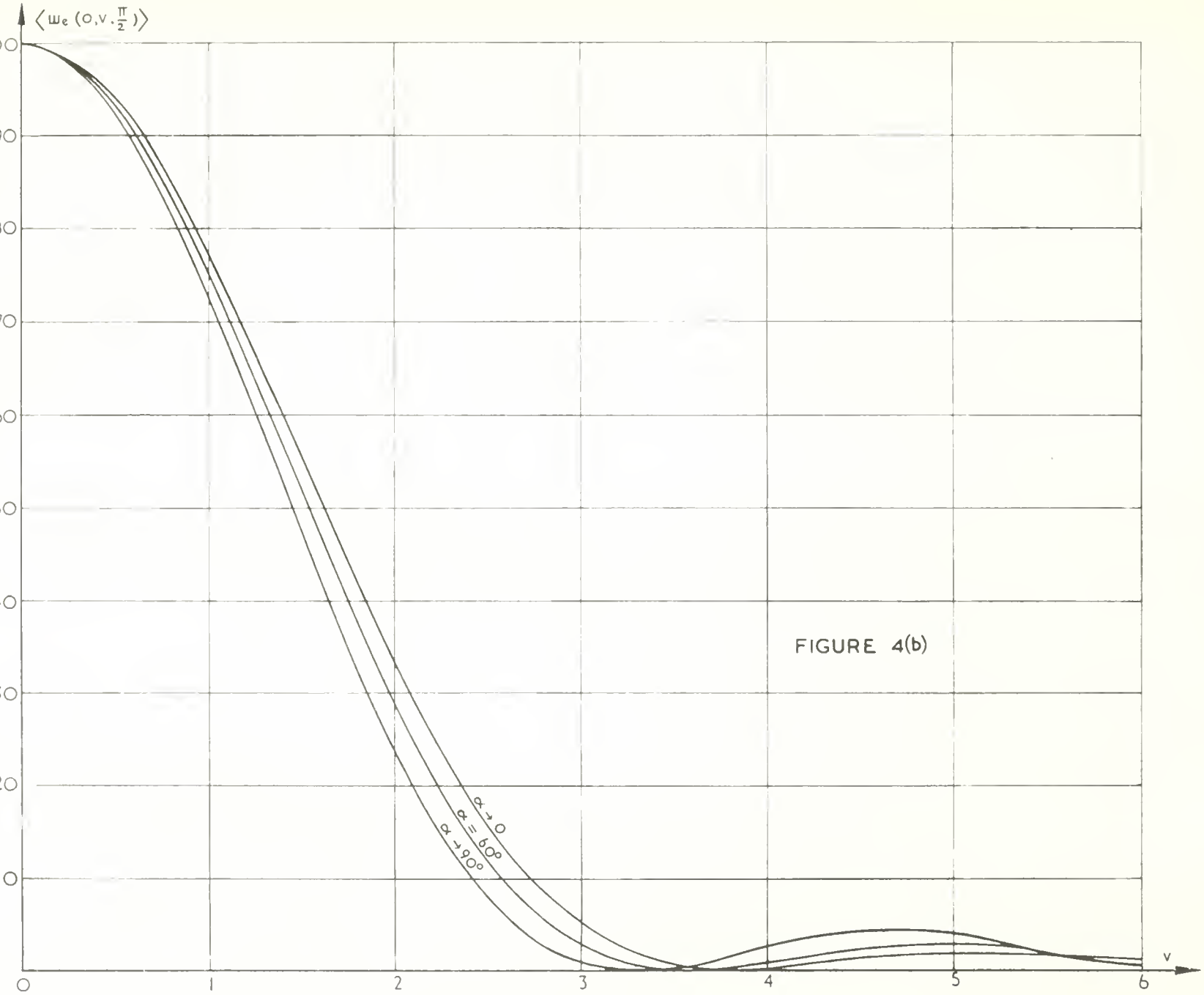
$\langle w_e(0,v,\frac{\pi}{2})\rangle$
100
90
80
70
60
50
40
30
20
10
0
1
2
3
4
5
6
v
$\alpha \to 0$
$\alpha = 60°$
$\alpha \to 90°$

FIGURE 4(b)

On substituting from (2.30) and (2.31) into (3.20), we obtain the following expressions for the components of $\langle \vec{S} \rangle$:

$$(3.21)\quad \begin{cases} \langle S_x \rangle = \dfrac{cA^2}{4\pi} \cos\phi \, \mathcal{Q}\left\{ I_1 \, (I_2^* - I_o^*) \right\} , \\ \langle S_y \rangle = \dfrac{cA^2}{4\pi} \sin\phi \, \mathcal{Q}\left\{ I_1 \, (I_2^* - I_o^*) \right\} , \\ \langle S_z \rangle = \dfrac{cA^2}{8\pi} \left\{ |I_o|^2 - |I_2|^2 \right\}, \end{cases}$$

where $\mathcal{Q}$ denotes the imaginary part.

We see that the magnitude of the time averaged Poynting vector is given by

$$(3.22)\quad |\langle \vec{S} \rangle| = \frac{cA^2}{8\pi} \left\{ (|I_o|^2 - |I_2|^2)^2 + 4(\mathcal{Q}[I_1(I_2^* - I_o^*)]^2 \right\}^{(1/2)} .$$

Since this expression is independent of the azimuth ϕ, <u>the loci of constant $|\langle \vec{S} \rangle|$ are surfaces of revolution about the axis of the system</u>.

<u>Along the axis of revolution</u> of the system in the image space ($v = 0$) (3.22) reduces to

$$(3.23)\quad |\langle \vec{S} \rangle| = \frac{cA^2}{8\pi} \, | \, I_o \, (u,o) \, |^2 ;$$

On comparison with (3.17) we see that the relation $|\langle \vec{S} \rangle| = c\langle w \rangle$ holds at all points on the axis.

From (3.21) we readily deduce that <u>at each point in the image space the Poynting vector lies in the meridional plane which contains that point</u>, and that it makes an angle γ with the positive z-axis, given by

$$(3.24)\quad \begin{cases} \sin\gamma = \dfrac{2\left|\mathcal{Q}\left\{I_1\,(I_2^{*} - I_1^{*})\right\}\right|}{\left[\left(|I_o|^2 - |I_2|^2\right)^2 + 4\left\{\mathcal{Q}\left[I_1\,(I_2^{*} - I_o^{*})\right]\right\}^2\right]^{(1/2)}}\,, \\[2ex] \cos\gamma = \dfrac{|I_o|^2 - |I_2|^2}{\left[\left(|I_o|^2 - |I_2|^2\right)^2 + 4\left\{\mathcal{Q}\left[I_1\,(I_2^{*} - I_o^{*})\right]\right\}^2\right]^{(1/2)}}\,. \end{cases}$$

Using the relations (3.3) we see from (3.22) that

$$(3.25)\qquad |\langle \vec{S}\,(-u,v,\phi)\rangle| = |\langle \vec{S}\,(u,v,\phi)\rangle|\,,$$

i.e. <u>the magnitude of the time averaged Poynting vector is symmetric with respect to the focal plane</u>. Further, from (3.24), we have $\sin\{\gamma(-u,v,\phi)\} = -\sin\{\gamma(u,v,\phi)\}$, $\cos\{\gamma(-u,v,\phi)\} = \cos\{\gamma(u,v,\phi)\}$, so that, for $u \neq 0$,

$$(3.26)\qquad \gamma(-u,v,\phi) = 2\pi - \gamma(u,v,\phi)\,.$$

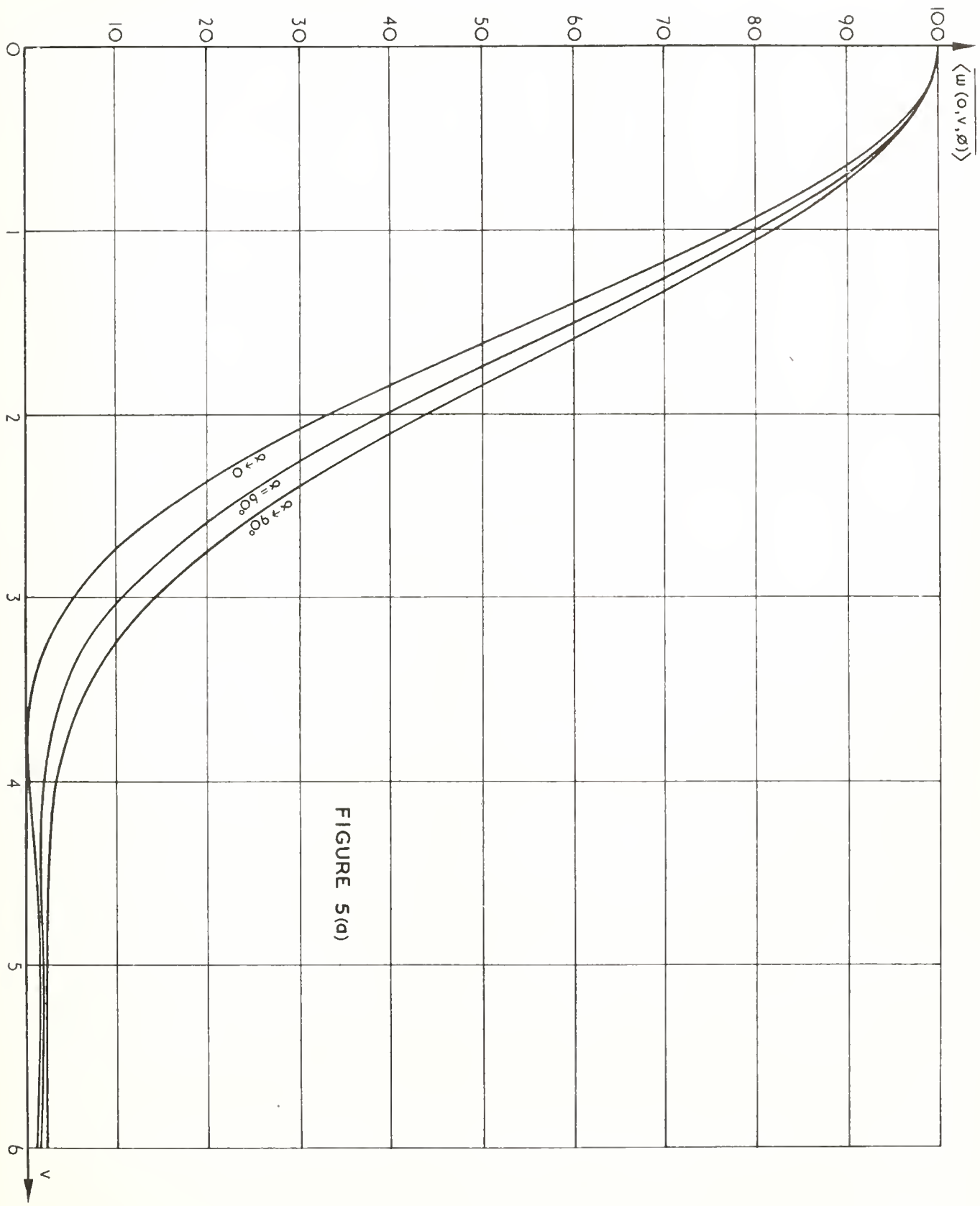

FIGURE 5(a)

For caption to Figures see page 41.

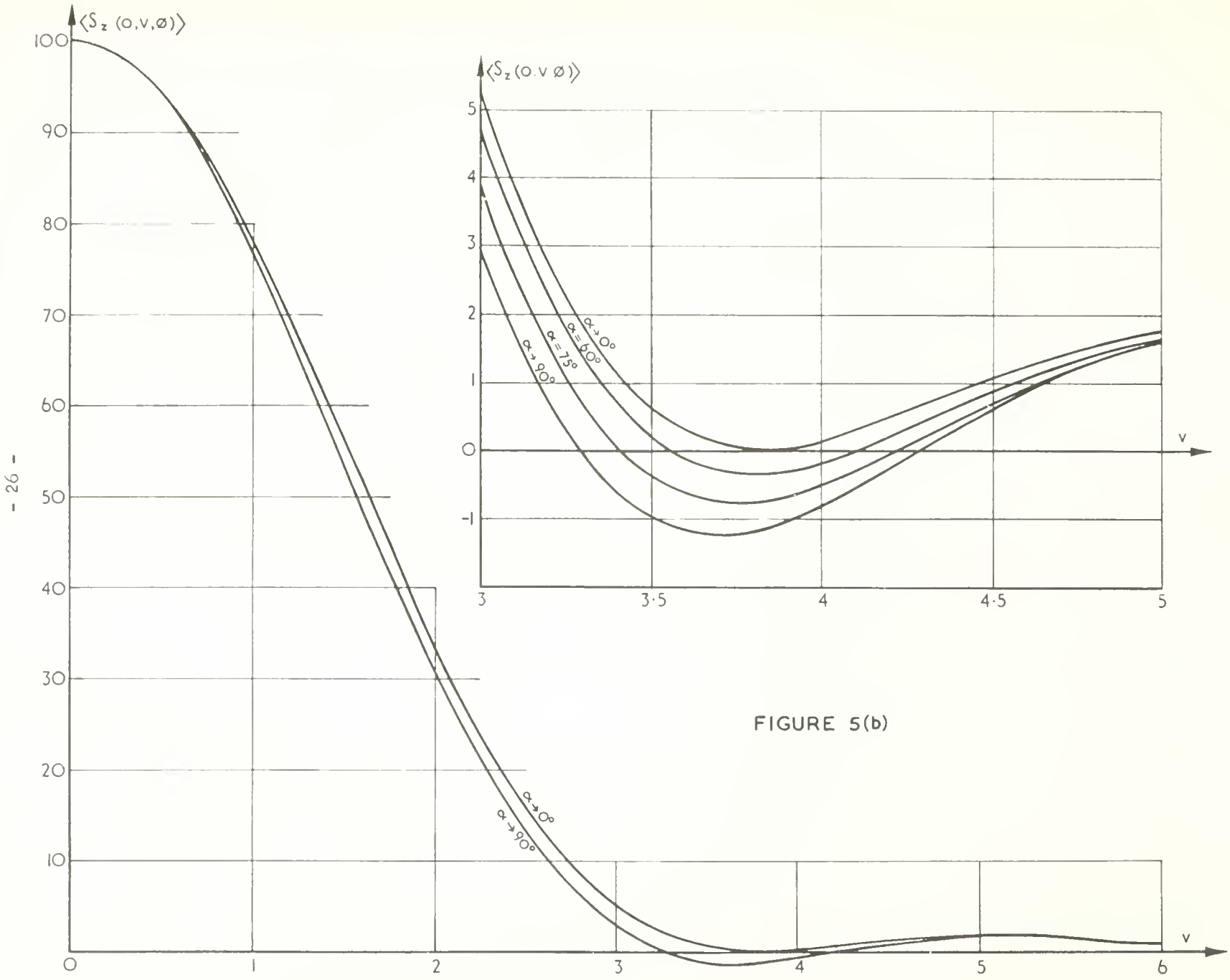
⟨Sz (o,v,ø)⟩
100
90
80
70
60
50
40
30
20
10
0
1
2
3
4
5
6
v
α→0°
α→90°
⟨Sz(o.v ø)⟩
5
4
3
2
1
0
-1
3
3·5
4
4·5
5
v
α→0°
α=60°
α=75°
α→90°

FIGURE 5(b)

When $u = 0$, we have from (3.21), since the integrals $I_n(o,v)$ $(n = 0, 1, 2)$ are all real,

$$(3.27) \qquad \langle S_x \rangle = \langle S_y \rangle = 0 ,$$

i.e. at any point in the focal plane, the time averaged energy flow, as represented by the Poynting vector is perpendicular to the focal plane. Moreover,

$$(3.28) \quad \begin{cases} \langle S_z \rangle > 0 \quad \text{if} \quad |I_o(o,v,)| > |I_2(o,v)| , \\ \text{and} \\ \langle S_z \rangle < 0 \quad \text{if} \quad |I_o(o,v)| < |I_2(o,v)| . \end{cases}$$

The second line implies that at points in the focal plane where $|I_2(0,v)| < |I_o(0.v)|$, the energy flow is directed back towards the object space.*

The computed curves, which show the behavior of $\langle S_z \rangle$ in the focal plane of aplanatic systems of selected angular semi-aperture α are shown in Figure 5. It is of interest to note that these (normalized) curves do nct substantially depend on α. In particular, in the region of the Rayleigh limit, where the durves do not drop below 0.8 of their respective maxima, the differences (for any particular v-value in this region) are less than 1 %, in the full range $(0 \leq \alpha \leq 90^\circ)$ of the angular semi-aperture.

---

*This interesting fact was already deduced by Ignatowsky (1919).

4. Approximate form of the solution for systems with a small angular aperture.

The structure of images in systems with small angular aperture is usually investigated on the basis of a scalar diffraction theory. The intensity distribution in the focal plane of an aberration-free system of revolution which images a point source was first determined in this way by Airy (1835). His analysis was extended by Lommel (1885) and Struve (1886), who determined the distribution in the whole three-dimensional neighborhood of the focus. It is of interest to examine the form which our solution takes when the angular semi-aperture α is small, and to compare it with these early solutions.

When α is small enough and u and v are not large compared with unity, we may replace the trigonometric factors in the amplitudes of the integrands in I_o, I_1 and I_2 in (3.2) by the leading term in their series expansions. In the exponents of the integrands we retain both the first and the second term in the expansion of cos θ since, when u is not small compared to unity, the contribution of the second term is evidently also significant. The integrals then become

$$(4.1)\quad \begin{cases} I_o(u,v) = 2 \exp\left[\dfrac{iu}{\alpha^2}\right] \displaystyle\int_o^\alpha \theta\, J_o\left(\frac{v\theta}{\alpha}\right) \exp\left[\frac{-iu\theta^2}{2\alpha^2}\right] d\theta\,, \\ I_1(u,v) = \exp\left[\dfrac{iu}{\alpha^2}\right] \displaystyle\int_o^\alpha \theta^2\, J_1\left(\frac{v\theta}{\alpha}\right) \exp\left[\frac{-iu\theta^2}{2\alpha^2}\right] d\theta\,, \\ I_2(u,v) = \dfrac{1}{2} \exp\left[\dfrac{iu}{\alpha^2}\right] \displaystyle\int_o^\alpha \theta^3\, J_2\left(\frac{v\theta}{\alpha}\right) \exp\left[\frac{-iu\theta^2}{2\alpha^2}\right] d\theta\,. \end{cases}$$

For small x, $J_n(x) \sim x^n$ and we see that I_1 and I_2 are of lower order in α than I_o, so that these integrals may be neglected in comparison with I_o. Hence (2.30) and (2.31) reduce to

$$e_x = h_y = - iAI_o \,, \tag{4.2}$$

$$e_y = e_z = h_x = h_z = 0 \,. \tag{4.3}$$

Thus in a system with a small angular aperture, the field in the image region is effectively linearly polarized; and the directions of the two field vectors in the image region are the same as their directions in the object space. We see that in this case the image field is completely specified by one (complex) scalar wave (e_x or h_y), which is represented by the integral I_o alone.

To evaluate I_o we introduce a new variable $\rho = \theta/\alpha$ and obtain

$$I_o(u,v) = 2\alpha^2 \exp\left[\frac{iu}{\alpha^2}\right] \int_0^1 \rho \, J_o(v\rho) \exp\left[-\frac{1}{2}iu\rho^2\right] d\rho \,. \tag{4.4}$$

The integral on the right may be evaluated in terms of two of the Lommel functions

$$U_n(u,v) = \sum_{s=0}^{\infty} (-1)^s \left(\frac{u}{v}\right)^{n+2s} J_{n+2s}(v) \,, \tag{4.5}$$

introduced by Lommel in the analysis already referred to.

In fact*

$$(4.6)\qquad \int_0^1 \rho\, J_o(v\rho)\, \exp\left[-\tfrac{1}{2} iu\rho^2 \right] d\rho = \frac{1}{u} \exp\left[-\tfrac{1}{2} iu \right] \left[U_1(u,v) + iU_2(u,v) \right]$$

From (4.2), (4.4) and (4.6) we obtain the following expressions for the only two non-vanishing field components in the image region

$$(4.7)\qquad e_x = h_y = -2iA\alpha^2 \frac{\exp\left[iu\left(\frac{1}{a^2} - \frac{1}{2} \right) \right]}{u} \left[U_1(u,v) + iU_2(u,v) \right]$$

The expressions (3.14) for the energy densities now become

$$(4.8)\qquad \langle w_e \rangle + \langle w_m \rangle = \tfrac{1}{2} \langle w \rangle = \frac{A^2}{16\pi} |I_o|^2 = \frac{A^2 \alpha^4}{4\pi} \frac{1}{u^2} \left[U_1^2(u,v) + U_2^2(u,v) \right]$$

---

*See Lommel (1885) or Born and Wolf (1959), § 8.8. The U_n-series converge for all u and v values, but are convenient for computations only when $|u/v| < 1$. When $|u/v| > 1$, (4.4) may be evaluated in terms of two of the Lommel's V_n-functions defined by

$$V_n(u,v) = \sum_{s=0}^{\infty} (-1)^s \left(\frac{v}{u} \right)^{n+2s} J_{n+2s}(v) .$$

The U and V-functions are related by means of the formula [cf. Watson, 1952, 537]

$$U_{n+1}(u,v) - (-1)^{n-1} V_{n-1}(u,v) = \sin\left\{ \tfrac{1}{2} u + \frac{v^2}{u} - n\pi \right\} .$$

The formulas (3.21) for the components of the Poynting vector become

$$(4.9) \qquad \langle S_x \rangle = \langle S_y \rangle = 0 ,$$

$$\langle S_z \rangle = \frac{cA^2}{8\pi} |I_o|^2 = \frac{cA^2\alpha^4}{2\pi} \frac{1}{u^2} \left[U_1^2(u,v) + U_2^2(u,v) \right] .$$

Thus, when α is small, the energy flow, as represented by the time averaged Poynting vector, is in the direction of the positive z-axis. On comparison of (4.8) and (4.9) we also see that the relation

$$(4.10) \qquad | \langle \vec{S} \rangle | = c \langle w \rangle$$

then holds everywhere in the image region.

The expressions on the right of (4.8) and (4.9) are proportional to the classical solution of Lommel and Struve for the 'intensity' in the image region of an aberration-free system.

When $u = 0$ (focal plane) we have from (4.7) since

$$\lim_{u \to 0} \frac{U_1(u,v)}{u} = \frac{J_1(v)}{v} , \qquad \lim_{u \to 0} \frac{U_2(u,v)}{u} = 0 ,$$

$$(4.11) \qquad e_x = h_y = - iA\alpha^2 \left(\frac{2J_1(v)}{v} \right)^2 ,$$

and (4.8) and (4.9) become

$$(4.12) \qquad \langle w_e \rangle = \langle w_m \rangle = \frac{1}{2} \langle w \rangle = \frac{1}{2c} | \langle \vec{S} \rangle | = \frac{A^2\alpha^4}{16\pi} \left(\frac{2J_1(v)}{v} \right)^2 .$$

The expression on the right of (4.12) is proportional to the classical solution of Airy for the 'intensity' in the image plane of an aberration-free system.

5. Images formed by an unpolarized wave

So far we have assumed that the wave entering the system is linearly polarized. We shall now briefly consider the case when the wave is unpolarized.

An unpolarized incident wave may become partially polarized on refraction (or on reflection) at the successive surfaces of the system. However, if the angles of incidence at each surface are small as is assumed, the degree of polarization introduced in this way will also be small and we may, therefore, consider the wave emerging from the system to be effectively unpolarized. If further, we assume that the wave is quasi-monochromatic, with mean angular frequency ω, the expressions for the time averaged energy densities and energy flow may be obtained by averaging the corresponding expressions relating to the polarized wave over all possible states of polarization.

To carry out this averaging it is convenient to choose a new set of coordinate axes $O\xi$, $O\eta$ at right angles to each other and to the axis of revolution. Let ϕ_o be the angle between $O\xi$ and the direction Ox of the electric vibrations of the incident wave, and let ϕ_P be the angle between $O\xi$ and the azimuth which contains the point P of observation (see Figure 6).

Then the first formula in (3.14) for the time average electric energy density at a point P of observation becomes, since $\phi = \phi_P - \phi_o$,

$$(5.1) \qquad \langle w_e \rangle = \frac{A^2}{16\pi} \left\{ |I_o|^2 + 4|I_1|^2 \cos^2(\phi_P - \phi_o) + |I_2|^2 + 2\cos\left[2(\phi_P - \phi_o)\right] \mathcal{R}(I_o I_2^*) \right\} .$$

If we denote by vertical bar an average over all possible values of $\phi_o (0 \leq \phi_o < 2\pi)$, it follows that when the incident wave is unpolarized

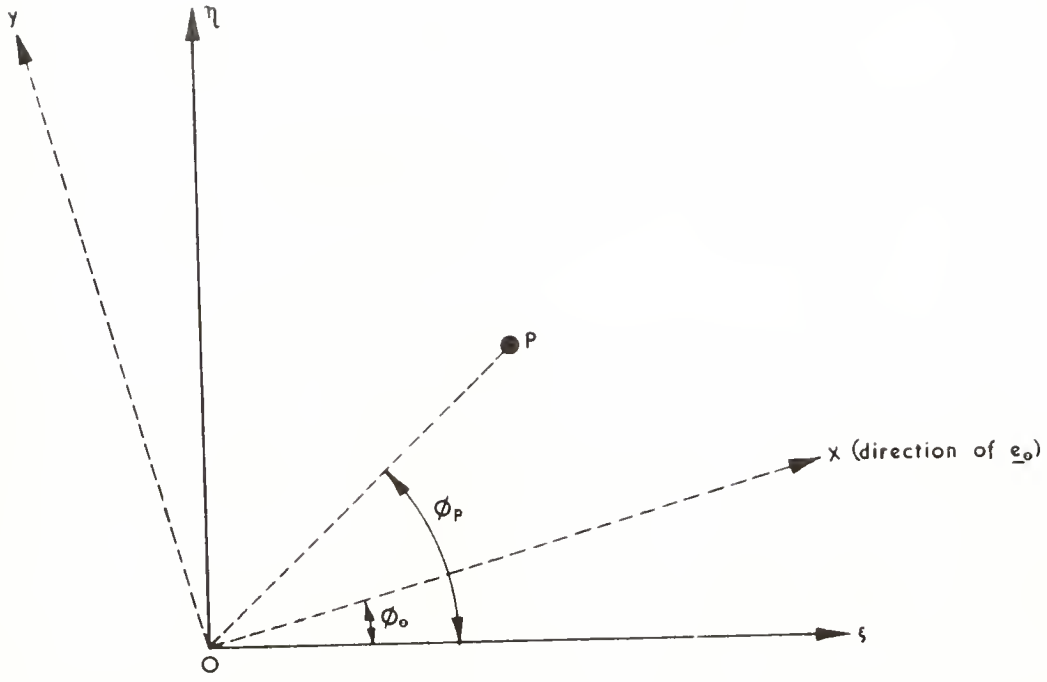

FIGURE 6

For caption to Figure see page 41.

the time averaged electric energy density at P is*

$$(5.2) \qquad \overline{\langle w_e \rangle} = \frac{1}{2\pi} \int_0^{2\pi} \langle w_e \rangle \, d\phi = \frac{A^2}{16\pi} \left\{ |I_o|^2 + 2|I_1|^2 + |I_2|^2 \right\} .$$

We note that $\overline{\langle w_e \rangle}$ is independent of ϕ_P so that the loci of the constant averaged electric energy are surfaces of revolution about the axis of the system, as was to be expected from symmetry. In a strictly similar manner, we obtain expressions for $\overline{\langle w_m \rangle}$ and $\overline{\langle w \rangle}$, and we have in all

$$(5.3) \qquad \overline{\langle w_e \rangle} = \overline{\langle w_m \rangle} = \frac{1}{2}\overline{\langle w \rangle} = \frac{A^2}{16\pi} \left\{ |I_o|^2 + 2|I_1|^2 + |I_2|^2 \right\} .$$

Comparison with the last expression in (3.14) shows that each term in (5.3) is also equal to one half of the total energy density of the polarized wave. The distribution of this quantity in the focal plane has already been given in Figure 5.

Next consider the energy flow. It is again convenient to transform first the expressions for the polarized case so that the coordinates which appear in them are referred to the fixed axes $O\xi$, $O\eta$, independent of the direction of polarization of the incident wave. Let $\langle S_\xi \rangle$ and $\langle S_\eta \rangle$ be the components of the time averaged Poynting vector in the directions $O\xi$, $O\eta$. Then

$$(5.4) \qquad \begin{cases} \langle S_\xi \rangle = \langle S_x \rangle \cos \phi_o - \langle S_y \rangle \sin \phi_o , \\ \langle S_\eta \rangle = \langle S_x \rangle \sin \phi_o + \langle S_y \rangle \cos \phi_o . \end{cases}$$

---

* The factor ℓ_o entering the constant $A = \pi f \ell_o / \lambda$ may now be related to the average electric energy density $\overline{\langle w_e \rangle}_i$ of the incident wave in the object space by means of the formula

$$\overline{\langle w_e \rangle}_i = \frac{1}{16\pi} (\vec{e}_o \cdot \vec{e}_o^{\,*}) = \frac{1}{16\pi} \ell_o^2 .$$

On substituting for $\langle S_x \rangle$ and $\langle S_y \rangle$ from (3.21), where again ϕ is replaced by $\phi - \phi_o$, we find that $\langle S_\xi \rangle$ and $\langle S_\eta \rangle$ are given by the same formulas as $\langle S_x \rangle$ and $\langle S_y \rangle$ but with ϕ_P written in place of ϕ. Since these formulas are independent of ϕ_o, they apply not only to the polarized wave but also to the unpolarized one, i.e.

$$(5.5a) \qquad \overline{\langle S_\xi \rangle} = \langle S_\xi \rangle = \frac{cA^2}{4\pi} \cos \phi_P \, \mathcal{Q} \left\{ I_1 (I_2^* - I_o^*) \right\},$$

$$(5.5b) \qquad \overline{\langle S_\eta \rangle} = \langle S_\eta \rangle = \frac{cA^2}{4\pi} \sin \phi_P \, \mathcal{Q} \left\{ I_1 (I_2^* - I_o^*) \right\}.$$

The remaining component, in the direction of the axis of revolution is, as before, given by the last formulas in (3.21),

$$(5.5c) \qquad \overline{\langle S_z \rangle} = \langle S_z \rangle = \frac{cA^2}{8\pi} \left\{ |I_o|^2 - |I_2|^2 \right\}.$$

It immediately follows that the results expressed by (3.22), (3.23) and (3.24) hold also for the unpolarized wave.

When the angular semi-aperture α is sufficiently small ($\alpha \to 0$) one may, as in § 4, neglect I_1 and I_2 in comparison with I_o. The above formulas then become, when (4.4) and (4.6) are used:

$$(5.6) \qquad \overline{\langle w_e \rangle} = \overline{\langle w_m \rangle} = \frac{1}{2} \overline{\langle w \rangle} = \frac{A^2 \alpha^4}{4\pi} \frac{1}{u^2} \left[U_1^2(u,v) + U_2^2(u,v) \right],$$

$$(5.7a) \qquad \overline{\langle S_\xi \rangle} = \overline{\langle S_\eta \rangle} = 0,$$

$$(5.7b) \qquad \overline{\langle S_z \rangle} = \frac{cA^2 \alpha^4}{2\pi} \frac{1}{u^2} \left[U_1^2(u,v) + U_2^2(u,v) \right].$$

Here U_1 and U_2 are again two of the functions defined by (4.5).

For points of observation in the focal plane ($u = 0$) these formulas reduce to

$$(5.8) \qquad \overline{\langle w_e \rangle} = \overline{\langle w_m \rangle} = \frac{1}{2}\overline{\langle w \rangle} = \frac{1}{2c}\,|\langle \vec{S} \rangle| = \frac{A^2\alpha^4}{16\pi}\left(\frac{2\,J_1(v)}{v}\right)^2 .$$

As already noted in connection with the corresponding formulas (4.8), (4.9) and (4.12), the quantities on the right hand sides of (5.6) and (5.7b) are proportional to the classical solution of Lommel and Struve for the 'intensity' in the image region of an aberration-free system, and the expression on the right hand side of (5.8) is proportional to the classical solution of Airy for the 'intensity' in the image plane.

Let us denote by suffix zero expressions (such as (5.6)) which refer to a low aperture system ($\alpha \to 0$) . Then from (4.8), (4.9),(5.3), (5.6) and (5.7) the following relations are seen to hold:

$$(5.9) \qquad \langle S_z \rangle_o = \overline{\langle S_z \rangle_o} = c\,\overline{\langle w \rangle_o} \leq c\,\overline{\langle w \rangle} = c\langle w \rangle ,$$

$$(5.10) \qquad \overline{\langle w_e \rangle_o} = \overline{\langle w_m \rangle_o} = \frac{1}{2}\overline{\langle w \rangle_o} \leq \frac{1}{2}\overline{\langle w \rangle} = \overline{\langle w_m \rangle} = \overline{\langle w_e \rangle} .$$

In practice, detectors of electric energy are usually used. The relation $\langle w_e \rangle_o \leq \langle w_e \rangle$ implies that the pattern recorded in any particular receiving plane ($u = \text{const}$) will then be broader in a system with a wide angular aperture than in one with a low angular aperture. For patterns in the focal plane, this effect is seen in Figure 5 which also shows that $\overline{\langle w_e \rangle}$ has no exact zeros, nor pronounced subsidiary maxima.

Finally, some of the main data which relate to the structure of the image in the focal plane of an aplanatic system are summarized in a Table below. Data relating to both polarized and unpolarized incident waves are given.

T A B L E

Value	Quantity	$\alpha \to 0$	$\alpha = 30^\circ$	$\alpha = 60^\circ$	$\alpha = 75^\circ$	$\alpha \to 90^\circ$
		v				
80	$\langle w_e(0,v,0)\rangle = \langle w_m(0,v,\frac{\pi}{2})\rangle$	0.93	0.98	1.16	1.33	1.48
	$\underline{\langle w_e(0,v,\frac{\pi}{2})\rangle = \langle w_m(0,v,0)\rangle}$	0.93	0.93	0.89	0.86	0.84
	$\underline{\langle w_e(0,v,\phi)\rangle = \langle w_m(0,v,\phi)\rangle}$	0.93	0.95	1.00	1.03	1.05
	$\langle S_z(0,v,\phi)\rangle = \langle S_z(0,v,\phi)\rangle$	0.93	0.93	0.93	0.93	0.91
60	$\langle w_e(0,v,0)\rangle = \langle w_m(0,v,\frac{\pi}{2})\rangle$	1.40	1.47	1.73	1.95	2.10
	$\underline{\langle w_e(0,v,\frac{\pi}{2})\rangle = \langle w_m(0,v,0)\rangle}$	1.40	1.38	1.32	1.30	1.26
	$\underline{\langle w_e(0,v,\phi)\rangle = \langle w_m(0,v,\phi)\rangle}$	1.40	1.42	1.50	1.55	1.58
	$\langle S_z(0,v,\phi)\rangle = \langle S_z(0,v,\phi)\rangle$	1.40	1.40	1.39	1.38	1.36
40	$\langle w_e(0,v,0)\rangle = \langle w_m(0,v,\frac{\pi}{2})\rangle$	1.83	1.94	2.27	2.50	2.63
	$\underline{\langle w_e(0,v,\frac{\pi}{2})\rangle = \langle w_m(0,v,0)\rangle}$	1.83	1.82	1.76	1.70	1.64
	$\underline{\langle w_e(0,v,\phi)\rangle = \langle w_m(0,v,\phi)\rangle}$	1.83	1.87	1.99	2.05	2.10
	$\langle S_z(0,v,\phi)\rangle = \langle S_z(0,v,\phi)\rangle$	1.83	1.83	1.82	1.82	1.79
20	$\langle w_e(0,v,0)\rangle = \langle w_m(0,v,\frac{\pi}{2})\rangle$	2.36	2.50	2.93	3.14	3.23
	$\underline{\langle w_e(0,v,\frac{\pi}{2})\rangle = \langle w_m(0,v,0)\rangle}$	2.36	2.33	2.22	2.16	2.10
	$\underline{\langle w_e(0,v,\phi)\rangle = \langle w_m(0,v,\phi)\rangle}$	2.36	2.41	2.56	2.66	2.73
	$\langle S_z(0,v,\phi)\rangle = \langle S_z(0,v,\phi)\rangle$	2.36	2.36	2.34	2.33	2.27
1st Min.	$\langle w_e(0,v,0)\rangle = \langle w_m(0,v,\frac{\pi}{2})\rangle$	3.83	4.15	4.75	4.75	4.70
	$\underline{\langle w_e(0,v,\frac{\pi}{2})\rangle = \langle w_m(0,v,0)\rangle}$	3.83	3.77	3.56	3.40	3.29
	$\underline{\langle w_e(0,v,\phi)\rangle = \langle w_m(0,v,\phi)\rangle}$	3.83	3.95	-	-	-
	$\langle S_z(0,v,\phi)\rangle = \langle S_z(0,v,\phi)\rangle$	3.83	3.80	3.80	3.76	3.70
2nd Min.	$\langle w_e(0,v,0)\rangle = \langle w_m(0,v,\frac{\pi}{2})\rangle$	7.02	7 03	8.10	8.10	8.00
	$\underline{\langle w_e(0,v,\frac{\pi}{2})\rangle = \langle w_m(0,v,0)\rangle}$	7.02	6.95	6.85	6.70	6.55
	$\underline{\langle w_e(0,v,\phi)\rangle = \langle w_m(0,v,\phi)\rangle}$	7.02	-	-	-	-
	$\langle S_z(0,v,\phi)\rangle = \langle S_z(0,v,\phi)\rangle$	7.02	7.02	7.02	7.02	6.95

Caption to Table is on page 42.

ACKNOWLEDGMENTS

The research described in this paper was carried our partly at New York University, when one of the authors (E.W.) was a guest of its Institute of Mathematical Sciences (Division of Electromagnetic Research), and partly at the University of Manchester, England.

The very extensive calculations on which the diagrams and the Table in this paper are based were carried out on the Manchester University Electronic Computor, Mark I. We are indebted to Mr. R.A. Brooker for helpful advice on computational techniques and to Miss B. Wood for help with construction of the contour diagrams shown in Figures 2 and 3.

REFERENCES

Airy, G.B.	1835,	Trans. Camb. Phil. Soc., 5 , 283.
Born, M. and Wolf, E.	1959,	'Principles of Optics' (London: Pergamon Press), In Press.
Burtin, R.	1956,	Optica Acta, 3 (1956), 104.
Carpenter, W.B.	1901,	'The Microscope and its Revelations'. (London: Churchill), 8th Ed.,p.381.
Focke, J.	1957,	Optica Acta, 4, 124.
Hopkins, H.H.	1943,	Proc. Phys. Soc. 55, 116.
-	1945,	Nature, London 155, 275.
Ignatowsky, B.C.	1919,	Trans. Opt. Inst. Petrograd, Vol.I, Paper IV.
-	1920,	Trans, Opt. Inst. Petrograd, Vol.I, Paper V.
Lommel, E.	1885,	Abh. Bayer. Akad. Wiss., 15, 233.
Richards, B.	1956a,	Contribution to 'Symposium on Astronomical Optics and Related Subjects' (ed. Z. Kopal, Amsterdam: North Holland Publishing Company), 352.
-	1956b,	Ph.D.Thesis, Univ. of Manchester.
Richards, B. and Wolf, E.	1956,	Proc. Phys. Soc. B., 69, 854.
Struve, H.	1886,	Mém. de l'Acad. de St. Petersbourgh, (7), 34, 1.
Watson, G.N.	1952,	'Treatise on the Theory of Bessel Functions'. (Cambridge University Press, 2nd. Ed.).
Wolf, E.	1958,	N.Y.U. Inst. Math. Sci., Div. E.M Res., Research Report No. EM-112, March 1958.

CAPTIONS TO FIGURES

Figure 1 : The meridional plane of a ray. The axis Ox is in the direction of the electric vector $\vec{e}_o$ in the object space.

Figure 2 : (a) Contours of $\chi(v,\phi)$, (b) Contours of $\rho(v,\phi)$. Polarization of the electric field in the focal plane of an aplanatic system of angular semi-aperture $\alpha = 60^\circ$ on the image side.

The field in the object space is linearly polarized with its electric vector in the azimuth $\phi = 0$. The field in the focal plane is, in general, elliptically polarized, with one axis (q) in the focal plane, and the other axis (p) perpendicular to the focal plane. $\chi(v,\phi)$ is the angle between the plane of the polarization ellipse of the electric vector and the meridional plane $\phi = 0$, and $\rho(v,\phi)$ is the ratio of the p and q axes. Radial distances are measured in v-units. The dotted lines indicate the dark rings of the Airy pattern represented by (4.12).

Figure 3 : Contours of the time averaged electric energy density $\langle w_e \rangle$ in the focal plane of an aplanatic system of angular semi-aperture α on the image side.

The field in the object space is linearly polarized with its electric vector in the azimuth $\phi = 0$. The crosses, dots and circles indicate maxima, minima and saddle points respectively. Radial distances are measured in v-units. The values are normalized to 100 at the focus. Figure (a), which represents the limiting case $\alpha \longrightarrow 0$ is identical with the classical intensity pattern of Airy, characterized by (4.12). The dotted circles in Figures (b) - (e) represent the dark rings in the Airy pattern.

Figure 4 : (a) Meridional section $\phi = 0$. (b) Meridional section $\phi = \frac{\pi}{2}$. The variation of the time averaged electric energy $\langle w_e \rangle$ along the two principal meridional section of the focal plane in an aplanatic system of selected angular semi-aperture α in the image space.

The field in the object space is linearly polarized with its electric vector in the azimuth $\phi = 0$. The values are normalized to 100 at the focus. The curves representing the limiting case $\alpha \rightarrow 0$ are identical with the classical Airy intensity curve given by (4.12).

Figure 5 : The variation of the time averaged total energy density (Figure a) and of the only non-vanishing component of the time averaged energy flow (Figure b) along any meridional section ϕ = const. of the focal plane of an aplanatic system of angular semi-aperture α on the image side. The curves represent the case of polarized as well as unpolarized wave. The curves in (a) also represent the variation of the time averaged electric and magnetic energy densities of an unpolarized wave. The values are normalized to 100 at focus.

Figure 6 : Change of reference system. Section at right angles to the axis of revolution.

Caption to Table

Comparison of data relating to the structure of the electromagnetic field in the focal plane ($u = 0$) of an aplanatic system of selected angular semi-aperture α on the image side.

$\langle w_e(u,v,\phi) \rangle$ and $\langle w_m(u,v,\phi) \rangle$ represent the time averaged electric energy density and magnetic energy density respectively. $\langle S_z \rangle$ represents the only non-vanishing component (in the direction of the axis of the system) of the time averaged energy flow. All the quantities are normalized to 100 at the focus $u = v = 0$.

Quantities with a vertical bar refer to an unpolarized wave, the others to linearly polarized wave in the object space, with its electric vector in the azimuth $\phi = 0$. The third row in each division of the table also represents one half of the time averaged total energy density $\langle w \rangle$, i.e.

$$\overline{\langle w_e \rangle} = \overline{\langle w_m \rangle} = \frac{1}{2}\overline{\langle w \rangle} = \frac{1}{2}\overline{\langle w \rangle} \quad .$$

The entries in the column $\alpha \longrightarrow 0$ are identical with values given by the intensity formulas (4.12) of Airy.

DISTRIBUTION LIST FOR RESEARCH REPORTS

Contract No. AF 19(604)5238

(ONE copy unless otherwise noted)

Commander
Air Research and Development Command
Andrews Air Force Base
Washington 25, D. C.
Attn: Major E. Wright, RDTCC

Director of Resident Training
3380th Technical Training Group
Keesler Air Force Base, Mississippi
Attn: OA-3011 Course

Director
Air University Library
Maxwell Air Force Base, Alabama

Commander
Air Force Missile Test Center
Patrick Air Force Base, Florida
Attn: MTE - for classified documents
Attn: MU-411, Technical Library - for unclassified documents

Tactical Air Group
Directorate of Research and Development
DCS/D
Headquarters, USAF
Washington, D. C.
Attn: Major R. L. Stell

Director, Communications and Electronics
Hq. U. S. Air Force
Washington 25, D. C.
Attn: AFOAC S/E

Commander
Wright Air Development Center
Wright-Patterson Air Force Base, Ohio
Attn: WCLRS-6, Mr. Portune

Wright Air Development Center
Wright-Patterson Air Force Base, Ohio
Flight Research Laboratory
Research Division
Attn: WCRRA

Commander
Wright Air Development Center
Wright-Patterson Air Force Base, Ohio
Attn: N. Draganjac, WCLNQ-4

Commander
Wright Air Development Center
Wright-Patterson Air Force Base, Ohio
Attn: Mr. Paul Springer, WCLRE-5

Commander
Air Technical Intelligence Center
Wright-Patterson Air Force Base, Ohio
Attn: ARCIN-4Bia

Commander
Rome Air Development Center
Griffiss Air Force Base, New York
Attn: RCSSTL-1

Commander
Rome Air Development Center
Griffiss Air Force Base, New York
Attn: Mr. Donald Dakan, RCUE

Commander
Rome Air Development Center (ARDC)
Griffiss Air Force Base, New York
Attn: Dr. John S. Burgess, RCE

Commander
Air Force Missile Development Center
Holloman Air Force Base, New Mexico
Attn: HDOIL, Technical Library

Director
U. S. Army Ordnance
Ballistic Research Laboratories
Aberdeen Proving Ground, Maryland
Attn: Ballistic Measurements Laboratory

Ballistic Research Laboratories
Aberdeen Proving Ground, Maryland
Attn: Technical Information Branch

Director
Evans Signal Laboratory
Belmar, New Jersey
Attn: Mr. O. C. Woodyard

U. S. Army Signal Engineering Labs.
Evans Signal Laboratory
Belmar, New Jersey
Attn: Technical Document Center

Massachusetts Institute of Technology
Signal Corps Liaison Officer
Cambridge 39, Mass.
Attn: A. D. Bedrosian, Room 26-131

Commanding General, SIGFM/EL-PC
U. S. Army Signal Engineering Labs.
Fort Monmouth, New Jersey
Attn: Dr. Horst H. Kedesdy
Deputy Chief, Chem-Physics Branch

Commander
Army Rocket and Guided Missile Agency
Redstone Arsenal, Alabama
Attn: Technical Library, ORDXR-OTL

Commanding General
U. S. Army Signal Engineering Labs.
Fort Monmouth, New Jersey
Attn: SIGFM/EL-AT

Department of the Army
Office of the Chief Signal Officer
Washington 25, D. C.
Attn: SIGRD-7

Office of Chief Signal Officer
Engineering and Technical Division
Washington 25, D. C.
Attn: SIGNET-5

Guided Missile Fuze Library
Diamond Ordnance Fuze Laboratories
Washington 25, D. C.
Attn: R. D. Hatcher, Chief Microwave
Development Section

(10) Armed Services Technical Information
Agency
Arlington Hall Station
Arlington 12, Virginia

(2) Library
Boulder Laboratories
National Bureau of Standards
Boulder, Coloredo

National Bureau of Standards
Department of Commerce
Washington 25, D. C.
Attn: Mr. A. G. McNish

National Bureau of Standards
Department of Commerce
Washington 25, D. C.
Attn: Gustave Shapiro, Chief
Engineering Electronics Section
Electricity and Electronics Div.

(2) Office of Technical Services
Department of Commerce
Washington 25, D. C.
Attn: Technical Reports Section
(Unclassified only)

Director
National Security Agency
Washington 25, D. C.
Attn: R/D (331)

(2) Hq. Air Force Cambridge Research Center
Laurence G. Hanscom Field
Bedford, Mass.
Attn: CROTLR-2 - P. Condon

(5) Hq. Air Force Cambridge Research Center
Laurence G. Hanscom Field
Bedford, Mass.
Attn: CROTLS - J. Armstrong

(5) Hq. Air Force Cambridge Research Center
Laurence G. Hanscom Field
Bedford, Mass.
Attn: CRRD

Director, Avionics Division (AV)
Bureau of Aeronautics
Department of the Navy
Washington 25, D. C.

Chief, Bureau of Ships
Department of the Navy
Washington 25, D. C.
Attn: Mr. E. Johnston, Code 833E

Commander
U. S. Naval Air Missile Test Center
Point Mugu, California
Attn: Code 366

U. S. Naval Ordnance Laboratory
White Oak
Silver Spring 19, Maryland
Attn: The Library

Commander
U. S. Naval Ordnance Test Station
China Lake, California
Attn: Code 753

Librarian
U. S. Naval Postgraduate School
Monterey, California

Air Force Development Field Representative
Naval Research Laboratory
Washington 25, D. C.
Attn: Code 1072

Director
U. S. Naval Research Laboratory
Washington 25, D. C.
Attn: Code 2027

Dr. J. I. Bohnert, Code 5210
U. S. Naval Research Laboratory
Washington 25, D. C. (Unclassified only)
Classified to be sent to:
Director
U. S. Naval Research Laboratory
Attn: Code 5200
Washington 25, D. C.

Commanding Officer and Director
U. S. Navy Underwater Sound Laboratory
Fort Trumbull, New London, Connecticut

Chief of Naval Research
Department of the Navy
Washington 25, D. C.
Attn: Code 427

Commanding Officer and Director
U. S. Navy Electronics Laboratory (Library)
San Diego 52, California

Chief, Bureau of Ordnance
Department of the Navy
Washington 25, D. C.
Attn: Code Ad3

Chief, Bureau of Ordnance
Department of the Navy
Surface Guided Missile Branch
Washington 25, D. C.
Attn: Code ReSl-e

Chief, Bureau of Ordnance
Department of the Navy
Washington 25, D. C.
Attn: Fire Control Branch (ReS4)

Department of the Navy
Bureau of Aeronautics
Technical Data Division, Code 4106
Washington 25, D. C.

Chief, Bureau of Ships
Department of the Navy
Washington 25, D. C.
Attn: Code 817B

Commanding Officer
U. S. Naval Air Development Center
Johnsville, Pennsylvania
Attn: NADC Library

Commander
U. S. Naval Air Test Center
Patuxent River, Maryland
Attn: ET-315, Antenna Branch

Director
Naval Ordnance Laboratory
Corona, California

Commanding Officer
U. S. Naval Ordnance Laboratory
Corona, California
Attn: Mr. W. Horenstein, Division 72

Airborne Instruments Laboratory, Inc.
160 Old Country Road
Mineola, New York
Attn: Dr. E. G. Fubini, Director
Research and Engineering Division

Aircom, Inc.
354 Main Street
Winthrop, Mass.

American Machine and Foundry Company
Electronics Division
1085 Commonwealth Avenue
Boston 15, Mass.
Attn: Mrs. Rita Moravcsik, Librarian

Andrew Alford, Consulting Engineers
299 Atlantic Avenue
Boston 10, Mass.

Avion Division
ACF Industries, Inc.
800 No. Pitt Street
Alexandria, Virginia
Attn: Library

Battelle Memorial Institute
505 King Avenue
Attn: Wayne E. Rife, Project Leader
Electrical Engineering Division
Columbus 1, Ohio

Bell Aircraft Corporation
Post Office Box One
Buffalo 5, New York
Attn: Eunice P. Hazelton, Librarian

Bell Telephone Laboratories, Inc.
Whippany Laboratory
Whippany, New Jersey
Attn: Technical Information Library

Pacific Division
Bendix Aviation Corporation
11600 Sherman Way
North Hollywood, California
Engineering Library
Attn: Peggie Robinson, Librarian

Bendix Radio Division
Bendix Aviation Corp.
E. Joppa Road
Towson 4, Maryland
Attn: Dr. D. M. Allison, Jr.
Director Engineering and Research

Boeing Airplane Company
Pilotless Aircraft Division
P.O. Box 3707
Seattle 24, Washington
Attn: R.R. Barber, Library Supervisor

Boeing Airplane Company
Wichita Division Engineering Library
Wichita 1, Kansas
Attn: Kenneth C. Knight, Librarian

Boeing Airplane Company
Seattle Division
Seattle 14, Washington
Attn: E.T. Allen, Library Supervisor

Bjorksten Research Labs, Inc.
P. O. Box 265
Madison, Wisconsin
Attn: Mrs. Fern B. Korsgard

Convair, A Division of General Dynamics Corp.
Fort Worth, Texas
Attn: K.G. Brown, Division Research Librarian

Convair, A Division of General Dynamics Corp.
San Diego 12, California
Attn: Mrs. Dora B. Burke,
Engineering Librarian

Cornell Aeronautical Laboratory, Inc.
4455 Genesee Street
Buffalo 21, New York
Attn: Librarian

Dalmo Victor Company
A Division of Textron, Inc.
1515 Industrial Way
Belmont, California
Attn: Mary Ellen Addems,
Technical Librarian

Dorne and Margolin, Inc.
29 New York Avenue
Westbury, Long Island, N. Y.

Douglas Aircraft Company, Inc.
P.O. Box 200
Long Beach 1, California
Attn: Engineering Library (C-250)

Douglas Aircraft Co., Inc.
827 Lapham Street
El Segundo, California
Attn: Engineering Library

Douglas Aircraft Company, Inc.
3000 Ocean Park Boulevard
Santa Monica, California
Attn: P.T. Cline
Eq. Sec. Reference Files,
Eq. Eng. A250

Douglas Aircraft Company, Inc.
2000 North Memorial Drive
Tulsa, Oklahoma
Attn: Engineering Library, D-250

Electronics Communication, Inc.
1830 York Road
Timonium, Maryland

Emerson and Cuming, Inc.
869 Washington Street
Canton, Mass.
Attn: Mr. W. Cuming

Emerson Electric Mfg. Co.
8100 West Florissant Avenue
St. Louis 21, Missouri
Attn: Mr. E.R. Breslin, Librarian

Sylvania Elec. Prod. Inc.
Electronic Defense Laboratory
P.O. Box 205 - (Uncl)
Mountain View, California
Attn: Library

Fairchild Aircraft Division
Fairchild Eng. and Airplane Corp.
Hagerstown, Maryland
Attn: Library

Farnsworth Electronics Company
3700 East Pontiac Street
Fort Wayne 1, Indiana
Attn: Technical Library

Federal Telecommunication Labs.
500 Washington Avenue
Nutley 10, New Jersey
Attn: Technical Library

The Gabriel Electronics
Division of the Gabriel Company
135 Crescent Road
Needham Heights 94, Mass.
Attn: Mr. Steven Galagan

General Electric Advanced Electronics Center
Cornell University
Ithaca, New York
Attn: J. B. Travis

General Electric Company
Electronics Park
Syracuse, New York
Attn: Documents Library, B. Fletcher
Building 3-143A

General Precision Laboratory, Inc.
63 Bedford Road
Pleasantville, New York
Attn: Mrs. Mary G. Herbst, Librarian

Goodyear Aircraft Corp.
1210 Massillon Road
Akron 15, Ohio
Attn: Library D/120 Plant A

Granger Associates
Electronic Systems
966 Commercial Street
Palo Alto, California
Attn: John V. N. Granger, President

Grumman Aircraft Engineering Corporation
Bethpage, Long Island, N. Y.
Attn: Mrs. A. M. Gray, Librarian
Engineering Library, Plant No. 5

The Hallicrafters Company
4401 West 5th Avenue
Chicago 24, Illinois
Attn: LaVerne LaGioia, Librarian

Hoffman Laboratories, Inc.
3761 South Hill Street
Los Angeles 7, California
Attn: Engineering Library

Hughes Aircraft Company
Antenna Department
Microwave Laboratory
Building 12, Room 2617
Culver City, California
Attn: M. D. Adcock

Hughes Aircraft Company
Florence and Teale Streets
Culver City, California
Attn: Dr. L.C. Van Atta, Associate Director
Research Labs.

Hycon Eastern, Inc.
75 Cambridge Parkway
Cambridge, Mass.
Attn: Mrs. Lois Seulowitz
Technical Librarian

International Business Machines Corp.
Military Products Division
590 Madison Avenue
New York 33, New York
Attn: Mr. C.F. McElwain, General Manager

International Business Machines Corp.
Military Products Division
Owego, New York
Attn: Mr. D. I. Marr, Librarian
Department 459

International Resistance Company
401 N. Broad Street
Philadelphia 8, Pa.
Attn: Research Library

Jansky and Bailey, Inc.
1339 Wisconsin Avenue, N. W.
Washington 7, D. C.
Attn: Mr. Delmer C. Ports

Dr. Henry Jasik, Consulting Engineer
298 Shames Drive
Brush Hollow Industrial Park
Westbury, New York

Electromagnetic Research Corporation
711 14th Street, N. W.
Washington 5, D. C.

Lockheed Aircraft Corporation
2555 N. Hollywood Way
California Division Engineering Library
Department 72-75, Plant A-1, Bldg. 63-1
Burbank, California
Attn: N. C. Harnois

The Martin Company
P. O. Box 179
Denver 1, Colorado
Attn: Mr. Jack McCormick

The Glenn L. Martin Company
Baltimore 3, Maryland
Attn: Engineering Library
Antenna Design Group

Maryland Electronic Manufacturing Corp.
5009 Calvert Road
College Park, Maryland
Attn: Mr. H. Warren Cooper

Mathematical Reviews
190 Hope Street
Providence 6, Rhode Island

The W. L. Maxson Corporation
460 West 34th Street
New York, N. Y.
Attn: Miss Dorothy Clark

McDonnell Aircraft Corporation
Lambert Saint-Louis Municipal Airport
Box 516, St. Louis 3, Missouri
Attn: R. D. Detrich, Engineering Library

McMillan Laboratory, Inc.
Brownville Avenue
Ipswich, Massachusetts
Attn: Security Officer. Document Room

Melpar, Inc. (2)
3000 Arlington Boulevard
Falls Church, Virginia
Attn: Engineering Technical Library

Microwave Development Laboratory
90 Broad Street
Babson Park 57, Massachusetts
Attn: N. Tucker, General Manager

Microwave Radiation Company Inc.
19223 South Hamilton Street
Gardena, California
Attn: Mr. Morris J. Ehrlich, President

Chance Vought Aircraft, Inc.
9314 West Jefferson Street
Dallas, Texas
Attn: Mr. H. S. White, Librarian

Northrop Aircraft, Inc.
Hawthorne, California
Attn: Mr. E. A. Freitas, Library Dept 3145
1001 E. Broadway

Remington Rand Univ. - Division of Sperry Rand Corporation
1900 West Allegheny Avenue
Philadelphia 29, Pennsylvania
Attn: Mr. John F. McCarthy
R and D Sales and Contracts

North American Aviation, Inc.
12214 Lakewood Boulevard
Downey, California
Attn: Engineering Library 495-115

North American Aviation, Inc.
Los Angeles International Airport
Los Angeles 45, California
Attn: Engineering Technical File

Page Communications Engineers, Inc.
710 Fourteenth Street, Northwest
Washington 5, D. C.
Attn: Librarian

Philco Corporation Research Division
Branch Library
4700 Wissachickon Avenue
Philadelphia 44, Pa.
Attn: Mrs. Dorothy S. Collins

Pickard and Burns, Inc.
240 Highland Avenue
Needham 94, Mass.
Attn: Dr. J. T. DeBettencourt

Polytechnic Research and Development Company, Inc.
202 Tillary Street
Brooklyn 1, New York
Attn: Technical Library

Radiation Engineering Laboratory
Main Street
Maynard, Mass.
Attn: Dr. John Ruze

Radiation, Inc.
P. O. Drawer 37
Melbourne, Florida
Attn: Technical Library, Mr. M.L. Cox

Radio Corp. of America
RCA Laboratories
Rocky Point, New York
Attn: P. S. Carter, Lab. Library

RCA Laboratories
David Sarnoff Research Center
Princeton, New Jersey
Attn: Miss Fern Cloak, Librarian
Research Library

Radio Corporation of America
Defense Electronic Products
Building 10, Floor 7
Camden 2, New Jersey
Attn: Mr. Harold J. Schrader
Staff Engineer, Organization
of Chief Technical
Administrator

The Ramo-Wooldridge Corporation
P.O. Box 45453 Airport Station
Los Angeles 45, California
Attn: Margaret C. Whitnah,
Chief Librarian

Hoover Microwave Co.
9592 Baltimore Avenue
College Park, Maryland

Director, USAF Project RAND
Via: Air Force Liaison Office
The Rand Corporation
1700 Main Street
Santa Monica, California

Rantec Corporation
Calabasas, California
Attn: Grace Keener, Office Manager

Raytheon Manufacturing Company
Missile Systems Division
Bedford, Mass.
Attn: Mr. Irving Goldstein

Raytheon Manufacturing Company
Wayland Laboratory, State Road
Wayland, Mass.
Attn: Mr. Robert Borts

Raytheon Manufacturing Company
Wayland Laboratory
Wayland, Mass.
Attn: Miss Alice G. Anderson,
Librarian

Republic Aviation Corporation
Farmingdale, Long Island, N. Y.
Attn: Engineering Library

Thru: Air Force Plant Representative
Republic Aviation Corp.
Farmingdale, Long Island, N.Y.

Rheem Manufacturing Company
9236 East Hall Road
Downey, California
Attn: J. C. Joerger

Trans-Tech, Inc.
P. O. Box 346
Frederick, Maryland

Ryan Aeronautical Company
Lindbergh Field
San Diego 12, California
Attn: Library - unclassified

Sage Laboratories
159 Linden Street
Wellesley 81, Mass.

Sanders Associates
95 Canal Street
Nashua, New Hampshire
Attn: N. R. Wild, Library

Sandia Corporation, Sandia Base
P.O. Box 5800, Albuquerque, New Mexico
Attn: Classified Document Division

Sperry Gyroscope Company
Great Neck, Long Island, New York
Attn: Florence W. Turnbull, Engr. Librarian

Stanford Research Institute
Menlo Park, California
Attn: Library, Engineering Division

Sylvania Electric Products, Inc.
100 First Avenue
Waltham 54, Mass.
Attn: Charles A. Thornhill, Report Librarian
Waltham Laboratories Library

Systems Laboratories Corporation
14852 Ventura Boulevard
Sherman Oaks, California
Attn: Donald L. Margerum

TRG, Inc.
17 Union Square West
New York 3, N. Y.
Attn: M. L. Henderson, Librarian

A. S. Thomas, Inc.
161 Devonshire Street
Boston 10, Mass.
Attn: A. S. Thomas, President

Bell Telephone Laboratories
Murray Hill
New Jersey

Chu Associates
P. O. Box 397
Whitcomb Avenue
Littleton, Mass.

Microwave Associates, Inc.
Burlington, Mass.

Raytheon Manufacturing Company
Missile Division
Hartwell Road
Bedford, Mass.

Radio Corporation of America
Aviation Systems Laboratory
225 Crescent Street
Waltham, Mass.

Lockheed Aircraft Corporation
Missile Systems Division Research Library
Box 504, Sunnyvale, California
Attn: Miss Eva Lou Robertson,
Chief Librarian

The Rand Corporation
1700 Main Street
Santa Monica, California
Attn: Dr. W. C. Hoffman

Commander
AF Office of Scientific Research
Air Research and Development Command
14th Street and Constitution Avenue
Washington, D. C.
Attn: Mr. Otting, SRY

Westinghouse Electric Corp.
Electronics Division
Friendship Int'l Airport Box 746
Baltimore 3, Maryland
Attn: Engineering Library

Wheeler Laboratories, Inc.
122 Cutter Mill Road
Great Neck, New York
Attn: Mr. Harold A. Wheeler

Zenith Plastics Co.
Box 91
Gardena, California
Attn: Mr. S. S. Olesky

Library Geophysical Institute
of the University of Alaska
College
Alaska

University of California
Berkeley 4, California
Attn: Dr. Samuel Silver,
Prof. Engineering Science
Division of Elec. Eng. Electronics
Research Lab.

University of California
Electronics Research Lab.
332 Corv Hall
Berkeley 4, California
Attn: J. R. Whinnery

California Institute of Technology
Jet Propulsion Laboratory
4800 Oak Grove Drive
Pasadena, California
Attn: Mr. I. E. Newlan

California Institute of Technology
1201 E. California Street
Pasadena, California
Attn: Dr. C. Papas

Carnegie Institute of Technology,
Schenley Park
Pittsburgh 13, Pennsylvania
Attn: Prof. A. E. Heins

Cornell University
School of Electrical Engineering
Ithaca, New York
Attn: Prof. G. C. Dalman

University of Florida
Department of Electrical Engineering
Gainesville, Florida
Attn: Prof. M. H. Latour, Library

Library
Georgia Institute of Technology
Engineering Experiment Station
Atlanta, Georgia
Attn: Mrs. J.H. Crosland, Librarian

Harvard University
Technical Reports Collection
Gordon McKay Library, 303A Pierce Hall
Oxford Street, Cambridge 38, Mass.
Attn: Mrs. E.L. Hufschmidt, Librarian

Harvard College Observatory
60 Garden Street
Cambridge 39, Mass.
Attn: Dr. Fred L. Whipple

University of Illinois
Documents Division Library
Urbana, Illinois

University of Illinois
College of Engineering
Urbana, Illinois
Attn: Dr. P. E. Moyes, Department of
Electrical Engineering

The Johns Hopkins University
Homewood Campus
Department of Physics
Baltimore 18, Maryland
Attn: Dr. Donald E. Kerr

Sandia Corporation
Attn: Organization 1423
Sandia Base
Albuquerque, New Mexico

Applied Physics Laboratory
The Johns Hopkins University
8621 Georgia Avenue
Silver Spring, Maryland
Attn: Mr. George L. Seielstad

Massachusetts Institute of Technology
Research Laboratory of Electronics
Room 20B-221
Cambridge 39, Massachusetts
Attn: John H. Hewitt

Massachusetts Institute of Technology
Lincoln Laboratory
P. O. Box 73
Lexington 73, Mass.
Attn: Document Room A-229

University of Michigan
Electronic Defense Group
Engineering Research Institute
Ann Arbor, Michigan
Attn: J. A. Boyd, Supervisor

University of Michigan
Engineering Research Institute
Radiation Laboratory
Attn: Prof. K. M. Siegel
912 N. Main St.,
Ann Arbor, Michigan

University of Michigan
Engineering Research Institute
Willow Run Laboratories
Willow Run Airport
Ypsilanti, Michigan
Attn: Librarian

University of Minnesota
Minneapolis 14, Minnesota
Attn: Mr. Robert H. Stumm, Library

Northwestern University
Microwave Laboratories
Evanston, Illinois
Attn: R. E. Beam

Ohio State University Research Found.
Ohio State University
Columbus 10, Ohio
Attn: Dr. T.E. Tice
Dept. of Elec. Engineering

The University of Oklahoma
Research Institute
Norman, Oklahoma
Attn: Prof. C. L. Farrar, Chairman
Electrical Engineering

Polytechnic Institute of Brooklyn
Microwave Research Institute
55 Johnson Street
Brooklyn, New York
Attn: Dr. Arthur A. Oliner

Polytechnic Institute of Brooklyn
Microwave Research Institute
55 Johnson Street
Brooklyn, New York
Attn: Mr. A. E. Laemmel

Syracuse University Research Institute
Collendale Campus
Syracuse 10, New York
Attn: Dr. C. S. Grove, Jr.
Director of Engineering Research

The University of Texas
Elec. Engineering Research Laboratory
P. O. Box 8026, University Station
Austin 12, Texas
Attn: Mr. John R. Gerhardt
Assistant Director

The University of Texas
Defense Research Laboratory
Austin, Texas
Attn: Claude W. Horton, Physics Library

University of Toronto
Department of Electrical Engineering
Toronto, Canada
Attn: Prof. G. Sinclair

Lowell Technological Institute
Research Foundation
P. O. Box 709, Lowell, Mass.
Attn: Dr. Charles R. Mingins

University of Washington
Department of Electrical Engineering
Seattle 5, Washington
Attn: G. Held, Associate Professor

Stanford University
Stanford, California
Attn: Dr. Chodorow
Microwave Laboratory

Physical Science Laboratory
New Mexico College of Agriculture
and Mechanic Arts
State College, New Mexico
Attn: Mr. H. W. Haas

Brown University
Department of Electrical Engineering
Providence, Rhode Island
Attn: Dr. C. M. Angulo

Case Institute of Technology
Cleveland, Ohio
Attn: Prof. S. Seeley

Columbia University
Department of Electrical Engineering
Morningside Heights
New York, N. Y.
Attn: Dr. Schlesinger

McGill University
Montreal, Canada
Attn: Prof. G. A. Woonton
Director, The Eaton Electronics
Research Lab.

Purdue University
Department of Electrical Engineering
Lafayette, Indiana
Attn: Dr. Schultz

The Pennsylvania State University
Department of Electrical Engineering
University Park, Pennsylvania

University of Pennsylvania
Institute of Cooperative Research
3400 Walnut Street
Philadelphia, Pennsylvania
Attn: Dept. of Electrical Engineering

University of Tennessee
Ferris Hall
W. Cumberland Avenue
Knoxville 16, Tennessee

University of Wisconsin
Department of Electrical Engineering
Madison, Wisconsin
Attn: Dr. Scheibe

University of Seattle
Department of Electrical Engineering
Seattle, Washington
Attn: Dr. D. K. Reynolds

Wayne University
Detroit, Michigan
Attn: Prof. A. F. Stevenson

Electronics Research Laboratory
Illinois Institute of Technology
3300 So. Federal Street
Chicago 16, Illinois
Attn: Dr. Lester C. Peach
Research Engineer

Advisory Group on Electronic Parts
Room 103
Moore School Building
200 South 33rd Street
Philadelphia 4, Pennsylvania

Ionosphere Research Laboratory
Pennsylvania State College
State College, Pennsylvania
ATTN: Professor A. H. Waynick, Director

Institute of Mathematical Sciences
25 Waverly Place
New York 3, New York
ATTN: Librarian

Electronics Division
Rand Corporation
1700 Main Street
Santa Monica, California
ATTN: Dr. Robert Kalaba

National Bureau of Standards
Washington, D. C.
ATTN: Dr. W. K. Saunders

Applied Mathematics and Statistics Lab.
Stanford University
Stanford, California
ATTN: Dr. Albert H. Bowker

Department of Physics and Astronomy
Michigan State College
East Lansing, Michigan
ATTN: Dr. A. Leitner

University of Tennessee
Knoxville, Tennessee
ATTN: Dr. Fred A. Ficken

Lebanon Valley College
Annville, Pennsylvania
ATTN: Professor B.H. Bissinger

General Atomic
P. O. Box 608
San Diego 12, California
Attn: Dr. Edward Gerjuoy

Department of Physics
Amherst College
Amherst, Mass.
ATTN: Dr. Arnold Arons

California Institute of Technology
1201 E. California Street
Pasadena, California
ATTN: Dr. A. Erdelyi

Mathematics Department
Stanford University
Stanford, California
ATTN: Dr. Harold Levine

University of Minnesota
Minneapolis 14, Minnesota
ATTN: Professor Paul C. Rosenbloom

Department of Mathematics
Stanford University
Stanford, California
ATTN: Professor Bernard Epstein

Applied Physics Laboratory
The Johns Hopkins University
8621 Georgia Avenue
Silver Spring, Maryland
ATTN: Dr. B. S. Gourary

(2) Exchange and Gift Division
The Library of Congress
Washington 25, D. C.

Electrical Engineering Department
Massachusetts Institute of Technology
Cambridge 39, Mass.
ATTN: Dr. L. J. Chu

Nuclear Development Associates, Inc.
5 New Street
White Plains, New York
ATTN: Library

California Institute of Technology
Electrical Engineering
Pasadena, California
ATTN: Dr. Zohrab A. Kaprielian

Dr. Rodman Doll
311 W. Cross Street
Ypsilanti, Michigan

California Inst. of Technology
Pasadena, California
ATTN: Mr. Calvin Wilcox

(3) Mr. Robert Brockhurst
Woods Hole Oceanographic Institute
Woods Hole, Mass.

National Bureau of Standards
Boulder, Colorado
ATTN: Dr. R. Gallet

Dr. Solomon L. Schwebal
3689 Louis Road
Palo Alto, California

University of Minnesota
The University of Library
Minneapolis 14, Minnesota
ATTN: Exchange Division

Department of Mathematics
University of California
Berkeley, California
ATTN: Professor Bernard Friedman

Lincoln Laboratory
Massachusetts Institute of Technology
P. O. Box 73
Lexington 73, Massachusetts
ATTN: Dr. Shou Chin Wang, Room C-351

Melpar, Inc.,
3000 Arlington Boulevard
Falls Church, Virginia
ATTN: Mr. K. S. Kelleher, Section Head

Hq. Air Force Cambridge Research Center
Laurence G. Hanscom Field
Bedford, Mass.
ATTN: Mr. Francis J. Zucker, CRRD

Hq. Air Force Cambridge Research Center
Laurence G. Hanscom Field
Badford, Mass.
ATTN: Dr. Philip Newman, CRRK

Mr. N. C. Gerson
Trapelo Road
South Lincoln, Mass.

Dr. Richard B. Barrar
Systems Development Corp.
2400 Colorado Avenue
Santa Monica, California

Columbia University Hudson Laboratories
P.O. Box 239
145 Palisade Street, Dobbs Ferry, N. Y.
ATTN: Dr. N. W. Johnson

Institute of Fluid Dynamics
and Applied Mathematics
University of Maryland
College Park, Maryland
ATTN: Dr. Elliott Montroll

Department of Electrical Engineering
Washington University
Saint Louis 5, Mo.
ATTN: Professor J. Van Bladel

Department of the Navy
Office of Naval Research Branch Office
1030 E. Green Street
Pasadena 1, California

Brandeis University
Waltham, Mass.
ATTN: Library

General Electric Company
Microwave Laboratory
Electronics Division
Stanford Industrial Park
Palo Alto, California
ATTN: Library

Smyth Research Associates
3555 Aero Court
San Diego 3, California
ATTN: Dr. John B. Smyth

Electrical Engineering
California Institute of Technology
Pasadena, California
ATTN: Dr Georges G. Weill

Naval Research Laboratory
Washington 25, D. C.
ATTN: Henry J. Passerini, Code 5278A

Dr. George Kear
5 Culver Court
Orinda, California

Brooklyn Polytechnic
85 Livingston Street
Brooklyn, New York
ATTN: Dr. Nathan Marcuvitz

Department of Electrical Engineering
Brooklyn Polytechnic
85 Livingston Street
Brooklyn, New York
ATTN: Dr. Jerry Shmoys

Department of Mathematics
University of New Mexico
Albuquerque, New Mexico
ATTN: Dr. I. Kolodner

Mathematics Department
Polytechnic Institute of Brooklyn
Johnson and Jay Street
Brooklyn, New York
ATTN: Dr. Harry Hochstadt

Ballistics Research Laboratory
Aberdeen Proving Grounds
Aberdeen, Maryland
ATTN: Dr. Pullan Keats

Dr. Lester Kraus
4935 Whitehaven Way
San Diego, California

University of Minnesota
Institute of Technology
Minneapolis, Minnesota
Attn: Dean Athelston Spilhaus

Ohio State University
Columbus, Ohio
Attn: Prof. C. T. Tai
Department of Electrical Eng.

Naval Research Laboratories
Washington 25, D. C.
Attn: W. S. Ament, Code 5271

Naval Research Laboratory
Washington 25. D. C.
Attn: Dr. Leslie G. McCracken, Jr.
Code 3933A

Office of Naval Research
Department of the Navy
Attn: Geophysics Branch, Code 416
Washington 25, D. C.

Office of Chief Signal Officer
Signal Plans and Operations Division
Attn: SIGOL-2, Room 20
Com. Liaison Br., Radio Prop. Sect.
The Pentagon, Washington 25, D. C.

Defence Research Member
Canadian Joint Staff
2001 Connecticut Straet
Washington, D. C.

Central Radio Prop. Lab.
National Bureau of Standards
Attn: Technical Reports Library
Boulder, Colorado

U. S. Weather Bureau
U. S. Department of Commerce
Washington 25, D. C.
Attn: Dr. Harry Wexler

Federal Communications Commission
Washington 25, D. C.
Attn: Mrs. Barbara C. Grimes, Librarian

Upper Atmosphere Research Section
Central Radio Propagation Laboratory
National Bureau of Standards
Boulder, Colorado

Argonne National Laboratory
P.O. Box 299
Lemont, Illinois
Attn: Dr. Hoylande D. Young

Bell Telephone Labs.
Murray Hill, New Jersey
Attn: Dr. S. O. Rice, 3B - 203

Carnegie Institute of Washington
Dept. of Terrestrial Magnetism
5241 Broad Branch Road, N. W.
Washington 15, D. C.
Attn: Library

Georgia Tech Research Institute
225 N. Avenue, N. W.
Attn: Dr. James E. Boyd
Atlanta, Georgia

University of Maryland
College Park, Maryland
Attn: Dr. A. Weinstein
Institute of Fluid Dynamics

Massachusetts Institute of Technology
Lincoln Laboratory
P. O. Box 73
Lexington 73, Massachusetts
Attn: Prof. Radford, Division 3 Head

Willow Run Research Center
University of Michigan
Willow Run Airport
Ypsilanti, Michigan
Attn: Dr. C. L. Dolph

School of Engineering
New York University
University Heights
New York, New York

Shell Fellowship Committee of the
Shell Companies Foundation, Inc.
50 West 50th Street
New York 20, N. Y.
Attn: Mr. J. R. Janssen

Esso Research and Engineering Co.
P. O. Box 51
Linden, New Jersey
Attn: Mr. C. L. Brown, Manager

Union Carbide and Carbon Corp.
30 E. 42nd Street
New York 17, New York
Attn: Mr. L. E. Erlanson

Convair
San Diego 12, California
Attn: Mr. Marvin Stern

Bell Telephone Labs., Inc.
463 West Street
New York 13, N. Y.
Attn: Dr. Mervin J. Kelly

Engineering Library
University of California
405 Hilgard Avenue
Los Angeles 24, California

Convair, A Division of General Dynamics Corp.
Daingerfield, Texas
Attn: J. E. Arnold, Division Manager

Convair, A Division of General Dynamics Corp.
San Diego 12, California
Attn: R. L. Bayless, Chief Engineer

Convair, a Division of General Dynamics Corp.
San Diego 12, California
Attn: K. J. Bossart, Chief Engineer-WS107A

Convair, A Div. of General Dynamics Corp.
Fort Worth 1, Texas
Attn: F. W. Davis, Chief Engineer

Convair, A Div. of General Dynamics Corp.
Pomona, California
Attn: C. D. Parrine
Ass't Div. Manager, Engin.

Shell Development Company
Exploration and Production Res. Div.
3737 Bellaire Boulevard
Houston 25, Texas
Attn: Miss Aphrodite Mamoulides

RCA Laboratories
Princeton, New Jersey
Attn: Dr. Charles Polk

Stanford Research Institute
S. Pasadena, California
Attn: Dr. J. Brandstatten

Wayne State University
Kresge-Hooker Science Library
5250 Second Boulevard
Detroit 2, Michigan

ARRA
1 Bond Street
Westbury, L. I., New York
Attn: Dr. Norman Spector

Varian Associates
611 Hansen Way
Palo Alto, California
Attn: Mrs. Perry Conway
Technical Librarian

Case Institute of Technology
Department of Electrical Engin.
University Circle
Cleveland 6, Ohio
Attn: Prof. Robert Plonsey

Dr. Ming S. Wong, CRRKP
Air Force Cambridge Research Center
Laurence G. Hanscom Field
Bedford, Massachusetts

Physics Section
AVCO-RAD Division
20 South Union Street
Lawrence, Mass.
Attn: Dr. Ernest Bauer

Advanced Development Section
Western Development Labs.
Philco Corp.
3875 Fabian Way
Palo Alto, California
Attn: Dr. Albert R. Giddis

Department of Aeronautical Engineering
University of Michigan
Ann Arbor, Michigan
Attn: Prof. Mahinder Uberoi

Gordon McKay Laboratory
Harvard University
Cambridge 39, Mass.
Attn: Dr. S. R. Seshadri

Commander
Air Research and Development Command
Attn: RDTR
Andrews Air Force Base
Washington 25, D. C.

College of Engineering
Dept. of Electrical Engineering
University of Florida
Gainesville, Florida
Attn: Dr. Sullivan

Dr. V. M. Papadopoulos
Dept. of Engineering
Brown University
Providence, R. I.

Major Vernon Lee Dawson
RSDD-CML(MO)
Redstone Arsenal
Huntsville, Alabama

Grumman Aircarft Engineering Corp.
South Oyster Bay Road
Bethpage, Long Island, N. Y.
Attn: Dr. Charles Mack

AF Office of Scientific Research
Washington 25, D. C.
Attn: Dr. Karl Kaplan

University of California
Radiation Laboratory
P. O. Box 808
Livermore, California
Attn: Dr. Bernard A. Lippmann

Department of Electrical Engineering
Case Institute of Technology
University Circle
Cleveland 6, Ohio
Attn: Professor Albert E. Collin

Antenna Laboratory
Air Force Cambridge Research Center
Laurence G. Hanscom Field
Bedford, Massachusetts
Attn: Mr. Philip Blackstone

Lt. Mark J. Beran, CRRD
Air Force Cambridge Research Center
Laurence G. Hanscom Field
Bedford, Massachusetts

Mr. Richard Mack, CRRD
Air Force Cambridge Research Center
Laurence G. Hanscom Field
Bedford, Massachusetts

System Development Corporation
2500 Colorado Avenue
Santa Monica, California
Attn: Library

Date Due